nature communications

Article

https://doi.org/10.1038/s41467-025-55824-y

Multivalent S2 subunit vaccines provide broad protection against Clade 1 sarbecoviruses in female mice

Received: 3 April 2024

Accepted: 31 December 2024

Published online: 07 January 2025

Check for updates

Peter J. Halfmann[1,12], Raj S. Patel[2,12], Kathryn Loeffler[3], Atsuhiro Yasuhara[4], Lee-Ann Van De Velde[5], Jie E. Yang[6,7,8], Jordan Chervin[4], Chloe Troxell[4], Min Huang[4], Naiying Zheng[4], Elizabeth R. Wright[6,7,8], Paul G. Thomas[5], Patrick C. Wilson[4], Yoshihiro Kawaoka[1,9,10,11] ✉ & Ravi S. Kane[2,3] ✉

The continuing emergence of immune evasive SARS-CoV-2 variants and the previous SARS-CoV-1 outbreak collectively underscore the need for broadly protective sarbecovirus vaccines. Targeting the conserved S2 subunit of SARS-CoV-2 is a particularly promising approach to elicit broad protection. Here, we describe a nanoparticle vaccine displaying multiple copies of the SARS-CoV-1 S2 subunit. This vaccine alone, or as a cocktail with a SARS-CoV-2 S2 subunit vaccine, protects female transgenic K18-hACE2 mice from challenges with Omicron subvariant XBB as well as several sarbecoviruses identified as having pandemic potential including the bat sarbecovirus WIV1, BANAL-236, and a pangolin sarbecovirus. Challenge studies in female Fc-γ receptor knockout mice reveal that antibody-based cellular effector mechanisms play a role in protection elicited by these vaccines. These results demonstrate that our S2-based vaccines provide broad protection against clade 1 sarbecoviruses and offer insight into the mechanistic basis for protection.

More than four years have passed since the initial outbreak of the severe acute respiratory syndrome coronavirus 2 (SARS-CoV-2) virus and the resulting COVID-19 pandemic. SARS-CoV-2 is a sarbecovirus within the *Betacoronavirus* genus. The spike (S) protein facilitates the entry of the virus into host cells and has consequently been a common target for vaccine development. The S protein consists of the S1 and S2 subunits. The receptor binding domain (RBD) is found within the S1 region and binds to angiotensin-converting enzyme 2 (ACE-2) to initiate viral entry into host cells[1]. The S2 subunit subsequently undergoes conformational changes that lead to the fusion of the host cell and viral membranes[2].

The S1 subunit has been the primary target for antibodies elicited by licensed mRNA vaccines[3] (which encode the full S antigen) due to its immunodominance. However, the S1 subunit of the S protein is also its most variable subunit, and mutations in this region have enabled variants (particularly Omicron and its subvariants) to have increased ability to evade immunity from neutralizing antibodies elicited by these vaccines[4]. While recent vaccine efforts have been focused on

[1]Influenza Research Institute, Department of Pathobiological Sciences, School of Veterinary Medicine, University of Wisconsin, Madison, WI, USA. [2]Wallace H. Coulter Department of Biomedical Engineering, Georgia Institute of Technology, Atlanta, Georgia, USA. [3]School of Chemical & Biomolecular Engineering, Georgia Institute of Technology, Atlanta, Georgia, USA. [4]Drukier Institute for Children's Health, Department of Pediatrics, Weill Cornell Medicine, New York, NY, USA. [5]Department of Immunology, St. Jude Children's Research Hospital, Memphis, TN, USA. [6]Department of Biochemistry, University of Wisconsin, Madison, WI, USA. [7]Department of Biochemistry, Cryo-EM Research Center, University of Wisconsin, Madison, WI, USA. [8]Department of Biochemistry, Midwest Center for Cryo-Electron Tomography, University of Wisconsin, Madison, WI, USA. [9]Division of Virology, Department of Microbiology and Immunology, Institute of Medical Science, University of Tokyo, Tokyo, Japan. [10]The Research Center for Global Viral Diseases, National Center for Global Health and Medicine Research Institute, Tokyo, Japan. [11]Pandemic Preparedness, Infection and Advanced Research Center (UTOPIA), University of Tokyo, Tokyo, Japan. [12]These authors contributed equally: Peter J. Halfmann, Raj S. Patel. ✉e-mail: yoshihiro.kawaoka@wisc.edu; ravi.kane@chbe.gatech.edu

protecting against SARS-CoV-2 variants, there are also other more distant sarbecoviruses circulating in animals that have been identified as having pandemic potential[5,6] that may prove to be problematic in the future (Fig. 1). Taking this into account, while also considering the SARS-CoV-1 outbreak in 2003[7], there is an overall need for a vaccine that can protect against a broad range of sarbecoviruses.

There are many vaccines currently in development that seek to elicit broad protection against sarbecoviruses. Many of these strategies involve the use of mixtures of either the RBD[8–10] or the full S protein[11,12] from different sarbecoviruses to elicit a broadly protective antibody response. However, these vaccines primarily elicit protection against the S1 subunit, which is prone to mutations as seen from the variants mentioned above. Targeting the response to the S2 domain is a promising alternative approach to provide broad protection as this domain is much more conserved than the S1 subunit (Fig. 1c, d). Anti-SARS-CoV-2 S2 antibodies have also been shown to provide broad protection against not just SARS-CoV-2, but also MERS-CoV and SARS-CoV-1 in vivo[13]. To that end, we and others have designed vaccines that elicit a protective response targeting the S2 domain[14–20].

Ng et al. developed SARS-CoV-2 S2 DNA vaccines that elicited cross-reactive antibodies that bound to and neutralized endemic common cold coronaviruses, SARS-CoV-2 variants, and SARS-CoV-1 related sarbecoviruses. Mice vaccinated with two doses of this S2 vaccine were protected after separate ancestral and Alpha variant SARS-CoV-2 challenges[15]. Pang et al. developed a recombinant subunit vaccine focusing on the HR1 domain in the S2 subunit of the SARS-CoV-2 S protein[16,17]. Their vaccine elicited cross-neutralizing antibodies against SARS-CoV-2 Omicron variants in rabbits and rhesus macaques. Transgenic mice, hamsters, and rhesus macaques immunized with three doses of this vaccine were protected against the SARS-CoV-2 challenge. In addition, Syrian hamsters immunized three times with this vaccine were protected against a SARS-CoV-2 Omicron BA.2 challenge[16]. Kapingidza et al. engineered scaffolds displaying the SARS-CoV-2 S2 stem helix and conserved fusion-peptide adjacent epitopes as a vaccine[18]. While they did not evaluate protection solely using their S2-based vaccine, mice immunized twice with a spike mRNA vaccine and then boosted twice with their S2 construct were protected against a challenge with a bat sarbecovirus, WIV1. Hsieh et al. showed that mice immunized twice with their stabilized S2 vaccine protected BALB/c mice from a mouse-adapted SARS-CoV-2 challenge and partially protected from a mouse-adapted SARS-CoV-1 challenge[19]. Lee et al. reported that mice immunized with four doses of their stabilized S2 trimer vaccine were protected against an XBB.1.5 challenge[20].

Previously, we developed a protein-based SARS-CoV-2 vaccine where the S2 subunit was multivalently presented on virus-like particles (VLPs). We showed that our S2-based vaccine could elicit a

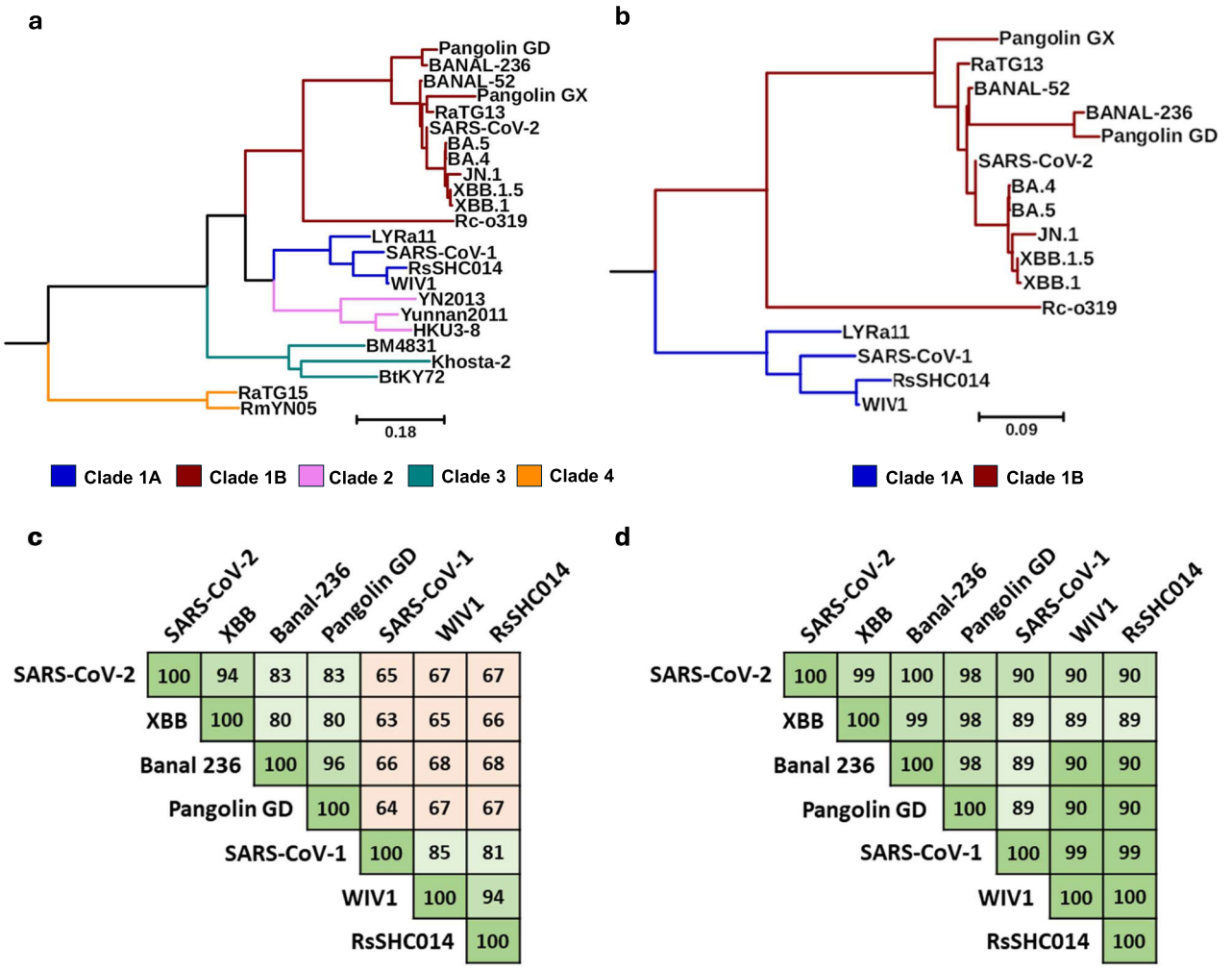

Fig. 1 | Analysis of Sarbecovirus Sequences. a Amino acid phylogenetic tree of selected Sarbecovirus S proteins. The scale bar represents the number of mutation events per residue. Clade assignments are indicated by branch and node color (Clade 1A: blue; Clade 1B: dark red; Clade 2: violet; Clade 3: teal; Clade 4: orange). **b** Amino acid phylogenetic tree of selected Sarbecoviruses S proteins from clade 1. Branch and node colors are the same as in Fig. 1a. **c** Sequence homology of selected clade 1 Sarbecovirus S1 subunits. **d** Sequence homology of selected clade 1 Sarbecovirus S2 subunits.

cross-reactive antibody response that recognized the spike proteins of not only SARS-CoV-2 variants, but also SARS-CoV-1 and the four endemic human coronaviruses[14]. Mice immunized with one dose of our S2 vaccine were protected against a mouse-adapted SARS-CoV-2 challenge. Moreover, hamsters immunized with three doses of our vaccine were protected against SARS-CoV-2 variants B.1.351 (Beta), B.1.617.2 (Delta), and BA.1(Omicron) as well as a pangolin coronavirus[14].

Overall, it is clear that vaccines based on the S2 region of the S protein are a promising path forward in developing a pan-sarbecovirus vaccine. SARS-CoV-2 is one of many viruses within the *Sarbecovirus* subgenus, that can be divided into 4 clades[21,22] (Fig. 1a). Clade 1 is split into two subclades[21] (Fig. 1b): Clade 1A which encompasses SARS-CoV-1 as well as other sarbecoviruses with pandemic potential[5,6], and Clade 1B which encompasses SARS-CoV-2 and related animal coronaviruses. Clade 1 contains all sarbecoviruses known to infect humans, and it is therefore important to design S2-based vaccines that provide broad protection against clade 1 sarbecoviruses. However, protection elicited by immunization solely with S2-based constructs against challenges has only been demonstrated against a limited number of clade 1 sarbecoviruses, primarily SARS-CoV-2 variants[14,15], a pangolin coronavirus in our previous work[14], and more recently a mouse-adapted SARS-CoV-1[19].

To that end, we further assessed the breadth of protection elicited by S2-based nanoparticle vaccines against various clade 1 A and clade 1B animal sarbecoviruses as well as mouse-adapted SARS-CoV-2 and XBB. Furthermore, we evaluated the protective efficacy of vaccines based on S2 antigens from both clade 1 A and clade 1B and investigated the mechanism of protection.

Specifically, we developed multivalent SARS-CoV-1 and bat-CoV RsSHC014 S2-based nanoparticle vaccines and showed that they (along with our previous SARS-CoV-2 S2 vaccine) significantly reduced virus titers in the lungs of immunized mice challenged with a mouse-adapted SARS-CoV-2 virus. We further evaluated the protective efficacy of the SARS-CoV-1 and SARS-CoV-2 S2 vaccines and found they significantly reduced virus titers in the lungs of immunized mice challenged with various clade 1 sarbecoviruses (XBB, BANAL-236, Pangolin-GD, W1V1, and RsSHC014) after a single dose. Immunized mice, challenged with mouse-adapted SARS-CoV-2 (MA10) had virus titers in the lungs that were not significantly different than similarly challenged mice after treatment with an anti-CD8 antibody, indicating that cytotoxic T cells do not play a major role in S2-based protection. In contrast, immunized Fc-gamma receptor (FcγR) knockout (KO) mice had significantly higher virus titers in the lungs compared to immunized wild-type mice when challenged with MA10, suggesting that cellular effector mechanisms played a role in S2-based protection. In addition, we evaluated our SARS-CoV-1 S2 vaccine and a vaccine containing both CoV-1 and CoV-2 S2 subunits against various sarbecoviruses in a prime-boost regimen. Mice immunized twice with these S2 vaccines showed no detectable virus in the lungs when challenged with Pangolin-GD and BANAL-236 and significantly reduced virus titers against mice challenged with WIV1 and XBB.

Results

Selection of S2 antigens for immunizations

As we were looking to generate vaccines that could protect against the entirety of Clade 1, we decided to evaluate S2 antigens based on sarbecoviruses in both Clade 1A and Clade 1B (Fig. 1b). For Clade 1A, we looked at the most prominent viruses present in that subclade. SARS-CoV-1 S2 (CoV-1 S2) was chosen due to the ability of SARS-CoV-1 to infect humans as seen from the 2003 outbreak[7]. Bat-CoV RsSHC014 S2 (SHC014 S2) was chosen because Bat-CoV RsSHC014 is one of the circulating clade 1A sarbecoviruses with pandemic potential[5]. Further Clade 1A candidates were not considered due to the high homology between the S2 subunits (Fig. 1d). For Clade 1B candidates, we opted to further evaluate our SARS-CoV-2 $S2_{mutS2'}$ construct (CoV-2 S2) due to its previous success in eliciting protection against clade 1B sarbecoviruses[14].

Generation and characterization of S2 vaccines

We have previously developed streptavidin-coated VLPs and multivalently presented numerous biotinylated antigens on them as vaccine constructs, including the Zika virus envelope protein domain III[23], Influenza virus hemagglutinin[24], various sarbecovirus S proteins[12,25], and the SARS-CoV-2 S2 subunit[14]. The core of the VLP is the bacteriophage MS2 coat protein, which self-assembles from 90 MS2 homodimers. An AviTag inserted into a surface loop of each dimer of the MS2 coat protein allows for site-specific biotinylation[12,14,23–25]. A solution containing the MS2 VLPs was added drop-wise to an excess of streptavidin; this mixture was further purified by size exclusion chromatography (SEC) to remove the excess streptavidin and recover the streptavidin-coated MS2 VLPs (MS2-SA).

All three selected S2 antigens were modified to include the HexaPro proline mutations[26] as well as mutations at the S2′ cut site, a C-terminal trimerization domain, a C-terminal AviTag for biotinylation, and a C-terminal his-tag for purification[14]. Plasmids encoding these constructs were transfected into Expi293F mammalian cells. The S2 antigens were purified by IMAC and SEC and then biotinylated in vitro. The S2 antigens were then mixed with MS2-SA to generate VLP-S2 constructs (Fig. 2a). The stoichiometric ratio of S2 antigen to MS2-SA was determined through analytical SEC, where the optimal ratio contained the least amount of MS2-SA without an SEC peak indicating any excess antigen[14].

The three S2 antigens (CoV-2 S2, CoV-1 S2, and SHC014 S2) were characterized by SDS polyacrylamide gel electrophoresis (SDS-PAGE), dynamic light scattering (DLS), and enzyme-linked immunosorbent assay (ELISA) individually, and then characterized again in the same manner after being multivalently displayed on MS2-SA. The VLP-S2 constructs were further characterized with negative stain transmission electron microscopy (NS-TEM). The SDS-PAGE gel showed the purity of the S2 and VLP-S2s (Fig. 2b). The DLS measurements showed that the VLP-S2s had diameters ranging from 75–85 nm, which was consistent with measured lengths of approximately 18–20 nm for the S2 antigens and 40–45 nm diameters for MS2-SA (Fig. 2c). The DLS measurement of the VLP-S2s was in a similar size range to previous characterizations[14]. Negative-stain transmission electron microscopy (NS-TEM) embeds the samples in a layer of dried heavy metal solution and provides fast and enhanced structural characterization with an increased signal-to-noise ratio (SNR)[27]. Here, like our previous reports[12,14,25], we applied NS-TEM to studies of S2 antigens attached to MS2-SA. Consistent with the biochemical analysis, the NS-TEM confirmed the incorporation of S2 protein on the surface of all VLP-S2s (Fig. 2d). The average diameters of the VLP-S2s were 75 nm, similar to DLS results. We next measured the binding of the S2-binding antibody S2P6 to the S2 and VLP-S2 proteins (Fig. 2e). All three S2s showed similar binding to the S2P6 antibody as soluble proteins and when displayed on MS2-SA, indicating that multivalent presentation doesn't interfere with S2 protein structure or folding.

VLP-S2 vaccines protect against a mouse-adapted SARS-CoV-2 challenge

We first evaluated the VLP-S2 vaccines against a challenge with a mouse-adapted strain of SARS-CoV-2 virus (MA10). Mice (C57BL/6, 10-12 week old, females; $n = 4$) were immunized once (prime) or twice (prime + boost) at a four-week interval with either VLP-CoV-2 S2, VLP-CoV-1 S2, VLP-SHC014 S2, or VLP-Control (MS2-SA) adjuvanted with AS03 and poly I:C. Four weeks after the last immunization, mice were intranasally inoculated with 10^5 plaque-forming units (pfu) of MA10. Three days after infection, lung tissue was collected, and virus titers were quantified by plaque assay (Fig. 3a).

https://doi.org/10.1038/s41467-025-55824-y

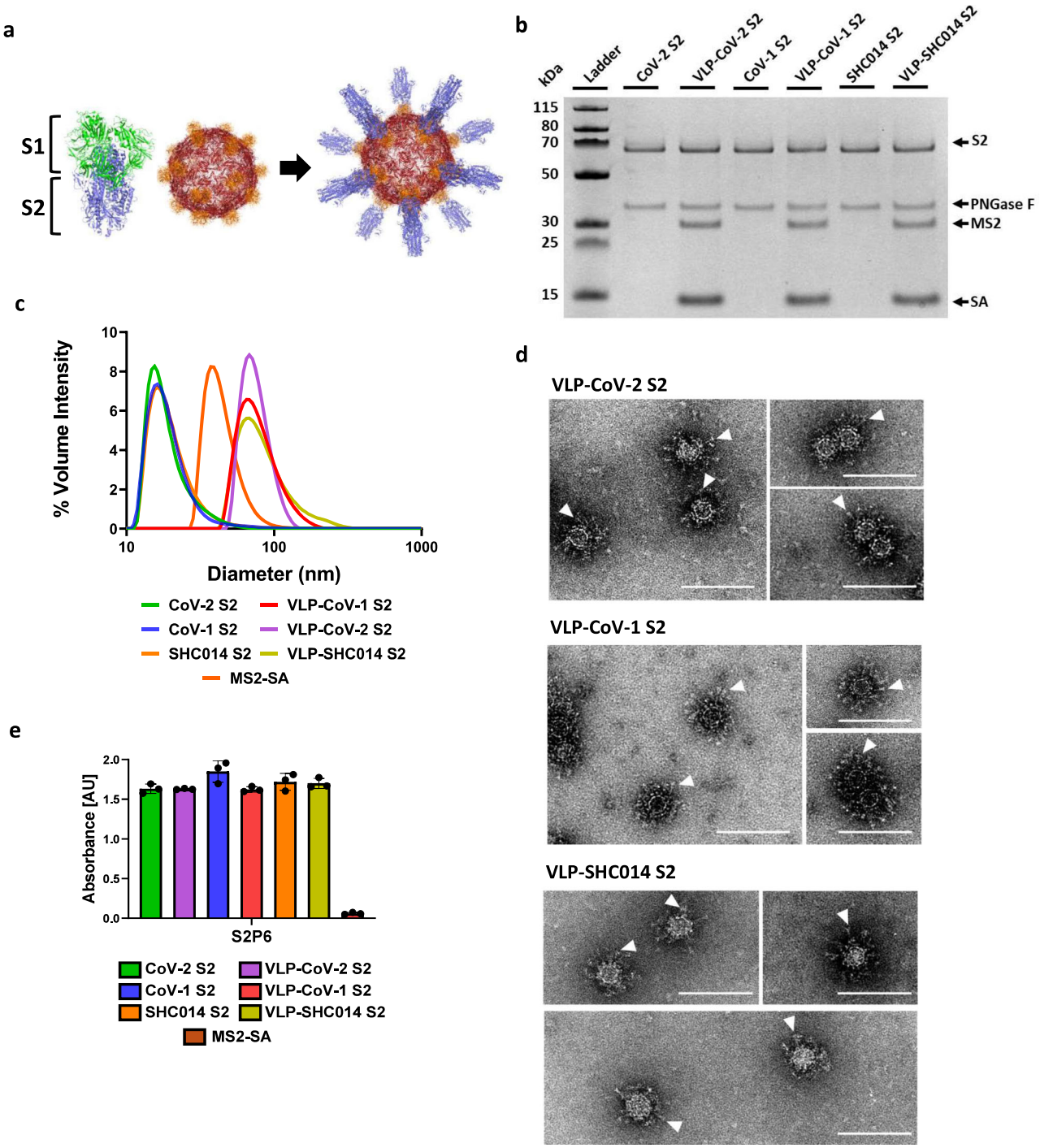

Fig. 2 | Characterization of S2 and VLP-S2. a Schematic of S protein and VLP-S2. **b** Characterization of S2 antigens and VLP-S2 by SDS-PAGE. Characterization by SDS-PAGE was performed twice using different preparations of each sample with similar results. **c** Characterization of S2, MS2-SA, and VLP-S2 by dynamic light scattering. **d** Representative negative-stain transmission electron micrographs of VLP-S2, scale bar = 100 nm. White arrowheads indicate the S2 protein on the VLP surface. The total number of examined images for VLP-CoV-2-S2, VLP-CoV-1-S2, and VLP-SHC014-S2 was 98, 74, and 96, respectively, from 3 independent experiments, with similar results. **e** Characterization of S2P6 antibody binding to S2 and VLP-S2 (mean ± SD, $n = 3$), one assay with three technical replicates.

Mice immunized with a single dose of the VLP-S2 vaccines had significantly lower virus titers in the lungs when compared to mice immunized with the VLP-Control (Fig. 3a). Compared to control mice, the mean virus titer in the lungs was more than 12,000-fold lower in VLP-CoV-2 S2 immunized mice, almost 10,000-fold lower in VLP-CoV-1 S2 immunized mice, and slightly over 2000-fold lower in VLP-SHC014 S2 immunized mice. Mice immunized with two doses of the VLP-S2s showed increased protection against MA10 compared to mice immunized with a single dose (Fig. 3a). The VLP-CoV-2 S2 and VLP-CoV-1 S2 immunized groups had 3 out of 4 mice with no detectable virus in the lungs, while the VLP-SHC014 S2 immunized group had 2 out of 4 mice with no detectable virus in the lungs. These results indicate that VLPs presenting either the Clade 1A S2 antigens or CoV-2 S2 provide comparable protection against an MA10 challenge. Despite this protection seen in mice immunized with the VLP-S2 vaccines, sera from immunized female C57BL/6 mice showed low neutralizing activity in vitro against an early SARS-CoV-2 isolate (Supplementary Fig. 1a), suggesting that the observed protection from virus challenge was not

https://doi.org/10.1038/s41467-025-55824-y

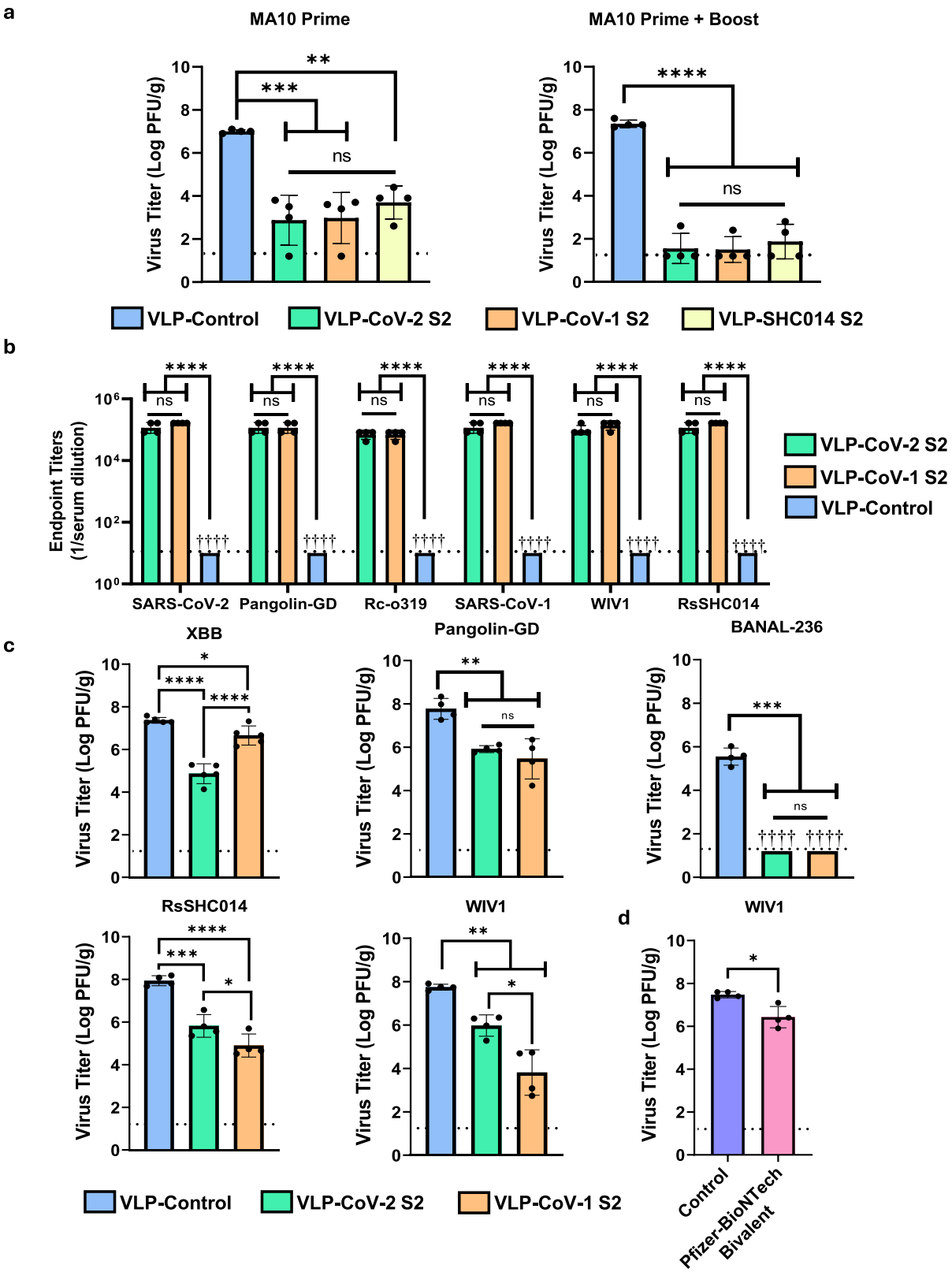

primarily based on antibody neutralization. We also characterized virus titers in the nasal turbinates after challenge (Supplementary Fig. 2a). Mice immunized with two doses of either VLP-CoV-1 S2 or VLP-CoV-2 S2 had almost 20-fold lower virus titers in the nasal turbinates compared to mice immunized with VLP-Control.

Since the difference in virus titers in the lungs between mice immunized with VLP-CoV-1 S2 and mice immunized with VLP-SHC014 S2 was not statistically significant (Fig. 3a), and since SARS-CoV-1 is the only clade 1A sarbecovirus known to infect humans, we further evaluated only the VLP-CoV-1 S2 and VLP-CoV-2 S2 vaccines.

VLP-S2 vaccines elicit cross-reactive antibodies in mice and protect against various clade 1 A and clade 1B sarbecoviruses after a single dose

To evaluate the cross-reactivity of the response, we characterized the overall IgG antibody response in C57BL/6 mice (10–12 week-old,

Fig. 3 | Protective efficacy of VLP-S2. a Lung virus titers of C57BL/6 mice immunized with S2 VLPs three days after mouse-adapted SARS-CoV-2 (MA10) challenge (mean ± SD, $n = 4$ biological replicates). $^{**}P = 0.0011$, $^{***}P < 0.001$ (VLP-Control vs VLP-CoV-2 S2: $P = 0.0002$; VLP-Control vs VLP-CoV-1 S2: $P = 0.003$), $^{****}P < 0.0001$, ns: not significant. ● indicate data from individual mice. The detection limit (dotted line) = 1.3 $\log_{10}$ pfu/g. Determined by ordinary one-way ANOVA and Tukey post hoc multiple comparisons between groups. **b** Antibody endpoint titers of sera from C57BL/6 mice immunized with S2 VLPs against spike proteins (geometric mean ± geometric SD, $n = 4$ biological replicates), $^{****}P < 0.0001$, ns: not significant, determined by Brown-Forsythe and Welch ANOVA and Games-Howell's multiple comparisons between groups for SARS-CoV-2, Pangolin-GD, SARS-CoV-1, and RsSHC014 S proteins, and by ordinary one-way ANOVA and Tukey post hoc multiple comparisons between groups for Rc-o319 and WIV1 S proteins. ● indicate data from individual mice**. c** Lung virus titers of K18-hACE2 mice immunized with S2 VLPs after infection with XBB, Pangolin-GD, BANAL-236, WIV1, and RsSHC014 (mean ± SD, $n = 5$ biological replicates for XBB and $n = 4$ for the rest). $^{*}P < 0.05$ (XBB challenge group VLP-Control vs VLP-CoV-1 S2: $P = 0.0298$; RsSHC014 challenge group VLP-CoV-2 S2 vs VLP-CoV-1 S2: $P = 0.0466$; WIV1 challenge group VLP-CoV-1 S2 vs VLP-CoV-2 S2: $P = 0.0390$), $^{**}P < 0.01$ (Pangolin-GD challenge group VLP-Control vs VLP-CoV-2 S2: $P = 0.0051$ and VLP-Control vs VLP-CoV-1 S2: $P = 0.0012$; WIV1 challenge group VLP-Control vs VLP-CoV-2 S2: $P = 0.0081$ and VLP-Control vs VLP-CoV-1 S2: $P = 0.0092$), $^{***}P < 0.001$ (BANAL-236 challenge group VLP-Control vs VLP-CoV-2 S2: $P = 0.0005$ and VLP-Control vs VLP-CoV-1 S2: $P = 0.0005$; RsSHC014 challenge group VLP-Control vs VLP-CoV-2 S2: $P = 0.0003$), $^{****}P < 0.0001$, WIV1 and BANAL-236 significance determined by Brown-Forsythe and Welch ANOVA and Games-Howell's multiple comparisons between groups, rest determined by ordinary one-way ANOVA and Tukey post hoc multiple comparisons between groups. The detection limit (dotted line) = 1.3 $\log_{10}$ pfu/g. ● or † indicate data from individual mice. † - No infectious virus was detected in the lungs. **d** Lung virus titers of K18-hACE2 mice immunized with Pfizer-BioNTech bivalent vaccine after infection with WIV1 (mean ± SD, $n = 4$ biological replicates). Significance determined by two-tailed Welch's t test, $^{*}P = 0.0201$. ● indicate data from individual mice.

females; $n = 4$) immunized with either VLP-CoV-1 S2 or VLP-CoV-2 S2 (Fig. 3b). Both VLP-S2 vaccines elicited high IgG antibody titers against the spike proteins from both clade 1A sarbecoviruses (SARS-CoV-1, WIV1, and RsSHC014) and clade 1B sarbecoviruses (SARS-CoV-2, Pangolin-GD, and bat-CoV Rc-o319). There was not a significant difference between endpoint IgG antibody titers elicited from VLP-CoV-1 S2 immunized mice compared to VLP-CoV-2 S2 immunized mice.

We next evaluated the ability of VLP-CoV-2 S2 and VLP-CoV-1 S2 to protect against challenges with XBB, Pangolin-GD, BANAL-236, RsSHC014, and WIV1 in K18-hACE2 transgenic mice (Fig. 3c). Mice (10–12 week old, females; $n = 4$-5) were immunized with a single dose of either vaccine or a VLP-Control and then challenged four weeks later with 10^5 pfu of the indicated challenge virus. For all five clade 1 sarbecoviruses tested in these challenge experiments, mice immunized with the VLP-S2 vaccines had virus titers in the lungs significantly lower than those for mice immunized with the VLP-Control (Fig. 3c) three days after the virus challenge. The most significant protection was seen against BANAL-236 (clade 1B bat sarbecovirus), where no infectious virus was detected in the lung tissue of mice immunized with either VLP-CoV-2 S2 or VLP-CoV-1 S2. Interestingly – as was the case for challenges with mouse-adapted SARS-CoV-2 (Fig. 3a) – there was no statistically significant difference in virus titers in the lung tissue between mice immunized with VLP-CoV-2 S2 and VLP-CoV-1 S2 when challenged with Pangolin-GD, another clade 1B sarbecovirus. These results indicate that CoV-1 and CoV-2 S2-based vaccines can provide broad protection against distant Clade 1 animal sarbecoviruses. However, mice immunized with VLP-CoV-2 S2 had significantly lower virus titers in the lungs when challenged with XBB compared to mice immunized with VLP-CoV-1 S2. XBB-challenged mice immunized with the VLP-CoV-2 S2 vaccine had a geometric mean virus titer in the lungs 320-fold lower than the mean virus titer of control mice, while mice immunized with the VLP-CoV-1 S2 vaccine had a geometric mean virus titer that was 5-fold lower. We also characterized viral titers in the nasal turbinates three days after challenge (Supplementary Fig. 2b). Mice immunized with VLP-CoV-2 S2 or VLP-CoV-1 S2 and challenged with Pangolin-GD showed a statistically significant reduction in virus titers in the nasal turbinates (45-fold and 61-fold, respectively) compared to virus titers in the control mice. XBB-challenged mice immunized with the VLP-CoV-2 S2 vaccine had a statistically significant 16-fold reduction in virus titers in the nasal turbinates compared to control immunized mice, while the 5-fold reduction for VLP-CoV-1-S2-immunized mice compared to control mice was not statistically significant. In infected K18-hACE mice, BANAL-236 did not replicate in the nasal turbinates even in the control immunized mice.

In the case of challenges with the clade 1A bat sarbecovirus RsSHC014, VLP-CoV-2 S2- immunized K18-hACE2 mice had geometric mean virus titers in the lungs that were approximately 130-fold lower than those in control mice, whereas VLP-CoV-1 S2 showed even lower virus titers, over 1000-fold lower than those for control mice. Similar results were seen for K18-hACE2 mice challenged with clade 1A bat sarbecovirus WIV1; VLP-CoV-2 S2-immunized mice had virus titers in the lungs almost 60-fold lower than control mice, whereas the VLP-CoV-1 S2-immunized mice had virus titers in the lungs almost 8600-fold lower than controls. For both clade 1A sarbecoviruses, mice immunized with the VLP-S2 vaccines had virus titers in the nasal turbinates significantly lower than those for mice immunized with the VLP-Control (Supplementary Fig. 2b). As another control, mice (K18-hACE, 10–12 week old, females; $n = 4$) were immunized with a single dose of the Pfizer-BioNTech bivalent mRNA vaccine (1 μg of vaccine) and challenged four weeks after immunization with 10^5 pfu of WIV1 (Fig. 3d). A small but statistically significant 12-fold decrease in virus titers in the lungs were seen compared to those of control mice immunized with PBS. No statistically significant difference in virus titers in the nasal turbinates of mice immunized with the bivalent mRNA vaccine was observed compared to control immunized mice (Supplementary Fig. 2c).

Since the VLP-CoV-1 S2 vaccine elicited comparable protection to the VLP-CoV-2 S2 vaccine against two of the three clade 1B sarbecovirus challenges and elicited significantly greater protection against both clade 1A sarbecoviruses, we used VLP-CoV-1 S2 to further evaluate the mechanism of protection.

$CD8^+$ T cells do not contribute significantly to protection elicited by VLP-CoV-1 S2 vaccine

To examine the role of $CD8^+$ cytotoxic T cells in S2-based protection, we tested the effect of depletion of $CD8^+$ T cells by treatment with an anti-CD8 depletion antibody (Supplementary Fig. 3) on protection elicited by VLP-CoV-1 S2 vaccine. Specifically, we treated groups of BALB/c mice (10–12 week-old females; $n = 4$-5) by intraperitoneal inoculation with either an anti-CD8 depletion antibody[28] or PBS. Treatments started three days and one day prior to immunization (day −3 and day −1), on the day of immunization (day 0), and after immunization (day +1, +3, +6, +9, and +12) (Fig. 4a). Both treated groups were immunized with the VLP-CoV-1 S2 vaccine. An additional control group was treated with PBS and immunized with the VLP-Control vaccine. Four weeks after immunization, all groups of mice were challenged with 10^5 pfu of MA10, and lung tissue was collected three days after the challenge. Both groups of VLP-CoV-1-S2-immunized mice showed significantly reduced virus titers in the lungs compared to control mice (Fig. 4b). There was, however, not a statistically significant difference in virus titers in the lungs between anti-CD8 antibody-treated, S2-immunized mice and PBS treated, S2-immunized mice, indicating that $CD8^+$ T cells do not play a significant role in protection elicited by immunization with VLP-CoV-1 S2. Similar results were observed with virus titers in the nasal turbinates.

https://doi.org/10.1038/s41467-025-55824-y

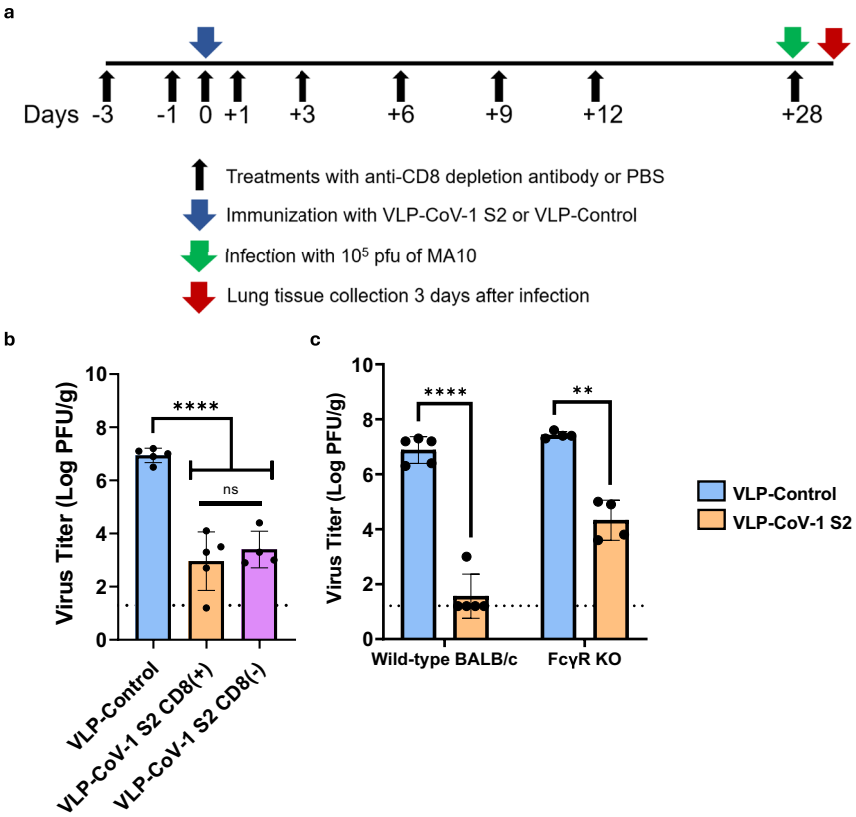

Fig. 4 | Probing the mechanism of S2-based protection. a Schedule for mouse pre-treatment with anti-CD8 antibody or PBS, immunization, infection with mouse-adapted SARS-CoV-2, and lung tissue collection. **b** Virus titers in the lungs of BALB/c mice immunized with VLP-CoV-1 S2 three days after mouse-adapted SARS-CoV-2 challenge (mean ± SD, $n = 5$ biological replicates for VLP-Control and S2 CD8(+) groups, $n = 4$ biological replicates for S2 CD8(-) group). ● indicate data from individual mice. The detection limit (dotted line) = 1.3 $\log_{10}$ pfu/g. The VLP-CoV-1 S2 CD8(+) group represents mice injected with PBS before the challenge, and the VLP-CoV-1 S2 CD8(-) group represents mice injected with CD8-depleting antibodies before the challenge. ****$P < 0.0001$, ns: not significant, determined by an ordinary one-way ANOVA and Tukey post hoc multiple comparisons between groups. **c** Virus titers in the lungs of mice immunized with VLP-CoV-1 S2 three days after MA10 challenge (mean ± SD, $n = 5$ biological replicates for wild-type BALB/c and $n = 4$ for FcγR KO). ● indicate data from individual mice. The detection limit (dotted line) = 1.3 $\log_{10}$ pfu/g. The FcγR KO group represents Fc-gamma receptor knocked out BALB/c mice. **$P = 0.0031$,****$P < 0.0001$, determined by two-tailed Welch's t test.

While both groups of VLP-CoV-1 S2 immunized mice had a statistically significant reduction in virus titers in the nasal turbinates compared to control mice, there was no significant difference in virus titers in the nasal turbinates between the two immunized groups (Supplementary Fig. 2d).

VLP-S2-immunized FcγR KO mice show increased virus titers in the lungs compared to wild-type immunized mice following a challenge with MA10

Previous reports suggest that Fc-mediated antibody effector functions may contribute to protection against SARS-CoV-2. Chen et al. found that sera from SARS-CoV-2 infected patients induced ADCC killing of SARS-CoV-2 target cells, primarily through the NK FcγRIIIa receptor (CD16)[29]. Tauzin et al. found plasma from individuals 3-weeks after being vaccinated with a single dose of the mRNA SARS-CoV-2 vaccine BNT162b2 had weak neutralizing but strong ADCC activity[30]. In addition, Yu et al. discovered patients who had severe disease and survived had sera that showed higher ADCC activity compared to patients who had severe disease and were deceased[31], indicating the potential importance of ADCC in protecting against severe SARS-CoV-2 infection. To determine whether antibody effector functions are involved in S2-based protection, two groups of FcγR KO BALB/c mice (10–12 week-old, females; $n = 4$) were immunized with a single dose of either VLP-CoV-1 S2 or VLP-Control and then challenged with MA10. Two groups of wild-type BALB/c mice (10–12 week old, females; $n = 5$) were similarly immunized and challenged with MA10 to serve as a comparison (Fig. 4c). While VLP-CoV-1 S2-immunized mice showed significantly lower virus titers in the lungs at three days after challenge compared to control mice in both wild-type and FcγR KO groups, a 160-fold greater reduction in mean viral lung titer relative to control was seen in the wild-type group. Wild-type mice immunized with VLP-CoV-1 S2 had a mean virus titer over 210,000-fold lower than that of control mice, and only 1 out of 5 immunized mice had any detectable virus in the lungs. In contrast, FcγR KO mice immunized with VLP-CoV-1 S2 had a mean virus titer approximately 1300-fold lower compared to control mice. These results suggest that antibody-dependent cell-based effector mechanisms play a critical role in the protection provided by immunization with VLP-CoV-1 S2. We saw evidence of the elicitation of neutralizing antibodies in female BALB/c mice after a single immunization with VLP-CoV-1 S2 (Supplementary Fig. 1b). While the neutralizing antibody titers are low, they could explain the observed reduction in lung viral titers even in FcγR KO mice. Consistent with the results of other challenge experiments, only a small but statistically significant difference was seen in nasal turbinate viral titers for immunized mice relative to controls (Supplementary Fig. 2e).

Characterization of B cells induced by VLP-S2 vaccines

We characterized B cell repertoires induced by the VLP-S2 vaccines using immunized mice. Groups of BALB/c mice (10–12 week old, females; $n = 5$) were subcutaneously inoculated with a single dose of

VLP-CoV-2 S2, VLP-CoV-1 S2, or VLP-Control. Four weeks post-immunization, splenocytes were harvested (Fig. 5a). IgG memory B cells binding to antigen fluorescent probes were sorted, followed by single-cell RNA sequencing (RNA-seq) and B cell receptor sequencing with a 10X platform. Antigen probes included ancestral-subunit proteins (RBD, NTD, or S2) and spike proteins derived from the SARS-CoV-2 omicron variant (XBB.1.5) or human CoVs (SARS-CoV-1, MERS-CoV, HKU1, OC43, or NL63). Since the antigen probes contained DNA oligonucleotide sequences, the antigen specificity of isolated B cells could be tracked. From antigen-specific B cells, a total of 348 pairs of immunoglobulin heavy and light chains were obtained.

To characterize immune induction by the VLP-S2 vaccines, we compared B cell repertoires obtained from BALB/c mice singly immunized with Wuhan-spike protein to the VLP-S2 vaccine repertoire. Based on binding intensities to subunit protein probes, we compared the epitope specificity of B cells induced by immunization. In Wuhan-spike immunized mice, RBD-binding B cells, NTD-binding B cells, and S2-binding B cells comprised 34, 11, and 55% of the total population respectively, whereas mice immunized with VLP-S2s (VLP-CoV-2 S2 or VLP-CoV-1 S2) only showed S2-binding B cells (Fig. 5b and Supplementary Fig. 4a). For S2-binding B cells in SARS-CoV-1 S2 VLP immunized mice since SARS-CoV-2 subunit probes were used in this experiment, the number of B cells cross-reacting to SARS-CoV-1 and SARS-CoV-2 are shown here. Antigen-specific B cells from each immunization group exhibited similar numbers of somatic mutations and lengths of complementarity-determining region 3 (CDR3) (Fig. 5c, d).

The probe binding profile for each B cell clone was determined next. (Fig. 5e–g). In VLP-CoV-2 S2-immunized mice, 78% of S2-binding B cells also bound to spike proteins derived from human CoVs (indicated by pink pie chart in Fig. 5e), while the remaining 22% showed SARS-CoV-2 specific binding (indicated by gray pie chart in Fig. 5e). Similarly, in VLP-CoV-1 S2-immunized mice, 88% of SARS-CoV-1 spike protein-binding B cells exhibited cross-reactivity with SARS-CoV-2 or other human CoV-derived spike proteins (Fig. 5f). These results confirm that B cells induced by the VLP-S2 vaccines possess broad cross-reactivity to coronaviruses. Data from Wuhan-spike immunized mice did not include probe binding data for XBB.1.5 and SARS-CoV-1 spike proteins, making comparison difficult, but only 32% of Wuhan-spike induced B cells cross-reacted with human CoV spike proteins (Fig. 5g). We summarized the number of bound strains and compared the cross-reactivity of B cells obtained from mice immunized with VLP-CoV-2 S2, VLP-CoV-1 S2, or Wuhan-Spike (Fig. 5h–j). Although a precise comparison cannot be made, it is evident that the breadth of the B cell response targeting the S2 domain was greater in the S2 VLP-immunized mice than in the Spike-immunized mice.

Monoclonal antibodies (mAbs) were generated from VLP-CoV-2 S2-immunized or VLP-CoV-1-immunized mice to characterize the breadth of binding using ELISA (Supplementary Table 1). M04A-061 and M04A-576 bound to spike proteins from SARS-CoV-2 variants (Delta, BA.4/5, BQ.1, XBB.1.5, or EG.5) and SARS-CoV-1 (Fig. 5k). M04A-520 and M04A-822 showed broader cross-reactivity, binding to multiple human CoVs. The binding specificity of monoclonal antibodies generally matched the B cell probe binding data, suggesting that the probe binding intensities represent B cell binding specificity. Furthermore, we investigated whether these antibodies possessed neutralizing potency using in vitro neutralization assay with SARS-CoV-2 spike pseudotyped virus (Fig. 5l). All antibodies showed no neutralizing activity against any pseudotyped virus (ancestral CoV-2-Spike, XBB.1.5-Spike, or SARS-CoV-1-Spike). To identify the epitopes of these four S2 mAbs, we performed competitive biolayer interferometry (BLI) with antibodies targeting the stem-helix (S2P6) or fusion peptide (COV44-62) (Supplementary Fig. 4b). These four mAbs did not compete with the reference antibodies, suggesting that these antibodies likely bind to other non-neutralizing epitopes.

We next investigated whether these mAbs activate the FcγR-mediated signaling pathway with antibody-dependent cellular cytotoxicity (ADCC) reporter bioassays (Fig. 5m). We found that all of our mAbs efficiently activated the ADCC signaling pathways in effector cells co-cultured with SARS-CoV-2 spike-expressing cells. These results indicate that our four anti-S2 mAbs have the potential to activate ADCC and are consistent with a role for effector-based mechanisms in protection suggested by the challenge experiments in FcγR KO mice (Fig. 4c). We also performed the ADCC reporter assay using serum from mice immunized with VLP-CoV-2 S2, VLP-CoV-1 S2, VLP-Control, or Wuhan-Spike (Supplementary Fig. 4c). In mice immunized with VLP-CoV-2 S2 and VLP-CoV-1 S2, ADCC activation was stronger compared to mice immunized with Wuhan-Spike.

VLP-S2 vaccines confer enhanced protection against clade 1A and clade 1B viruses in K18-hACE2 mice after prime-boost regimen

We next evaluated the protection provided by VLP-CoV-1 S2 using a prime-boost regimen in K18-hACE2 transgenic mice. In addition, considering that the VLP-CoV-1 S2 vaccine provided greater protection against clade 1A sarbecovirus challenges, and the VLP-CoV-2 S2 vaccine provided greater protection against an XBB challenge, we also evaluated whether a cocktail of VLP-CoV-1 S2 and VLP-CoV-2 S2 could provide a greater breadth of protection compared to VLP-CoV-1 S2 alone (Fig. 6). Mice (10–12 week old, females; $n = 5$/group) were immunized with either VLP-Control, VLP-CoV-1 S2, or a mixture of VLP-CoV-1 S2 and VLP-CoV-2 S2 and then boosted four weeks later. Four weeks after the second immunization, mice were challenged with 10^5 pfu of either Pangolin-GD, BANAL-236, WIV1, or XBB, and lung tissue was collected three days after the challenge. As seen with the single-dose immunizations, mice immunized with two doses of VLP-S2s all had significantly lower virus titers in the lungs when compared to mice immunized with the VLP-control. Mice immunized with two doses of the vaccine containing both S2 antigens had no detectable virus in the lungs when challenged with either Pangolin-GD or BANAL-236. Mice immunized with two doses of the VLP-CoV-1 S2 vaccine and challenged with BANAL-236 had no detectable virus in the lungs, similar to mice immunized with one dose. Mice immunized with two doses of the VLP-CoV-1 S2 vaccine and challenged with Pangolin-GD also had no detectable virus in the lungs, while mice previously immunized with a single dose of the same vaccine had only a ~ 200-fold reduction in the mean virus titer in the lungs. Overall, two doses of VLP-CoV-1 S2 or the VLP-S2 cocktail vaccine completely protected mice against challenges with these animal clade 1B sarbecoviruses, Pangolin-GD, and BANAL-236.

Mice immunized with 2 doses of VLP-CoV-1 S2 had virus titers in the lungs approximately 1200-fold lower than control following a challenge with WIV1. Mice immunized with two doses of the VLP-S2 cocktail vaccine had virus titers that were 6-fold-lower than VLP-CoV-1 S2-immunized mice – approximately 7200-fold lower than mice immunized with VLPs alone. For challenges with XBB, mice immunized with two doses of VLP-CoV-1 S2 showed a significant, nearly 150-fold reduction in titers in the lungs relative to controls. Once again, a greater, more than 1000-fold reduction in virus titers in the lungs relative to controls was seen for mice immunized with two doses of the VLP-S2 cocktail vaccine. These results indicate that a prime-boost regimen provides enhanced protection against challenges with clade 1 sarbecoviruses and that the inclusion of both clade 1A and clade 1B antigens in the vaccine enhances protection compared to a vaccine composed of a single S2 antigen. We also observed a statistically significant reduction in virus titers in the nasal turbinates of mice immunized with two doses of VLP-CoV-1 S2 or the VLP-S2 cocktail vaccine compared to control immunized mice (Supplementary Fig. 2f).

https://doi.org/10.1038/s41467-025-55824-y

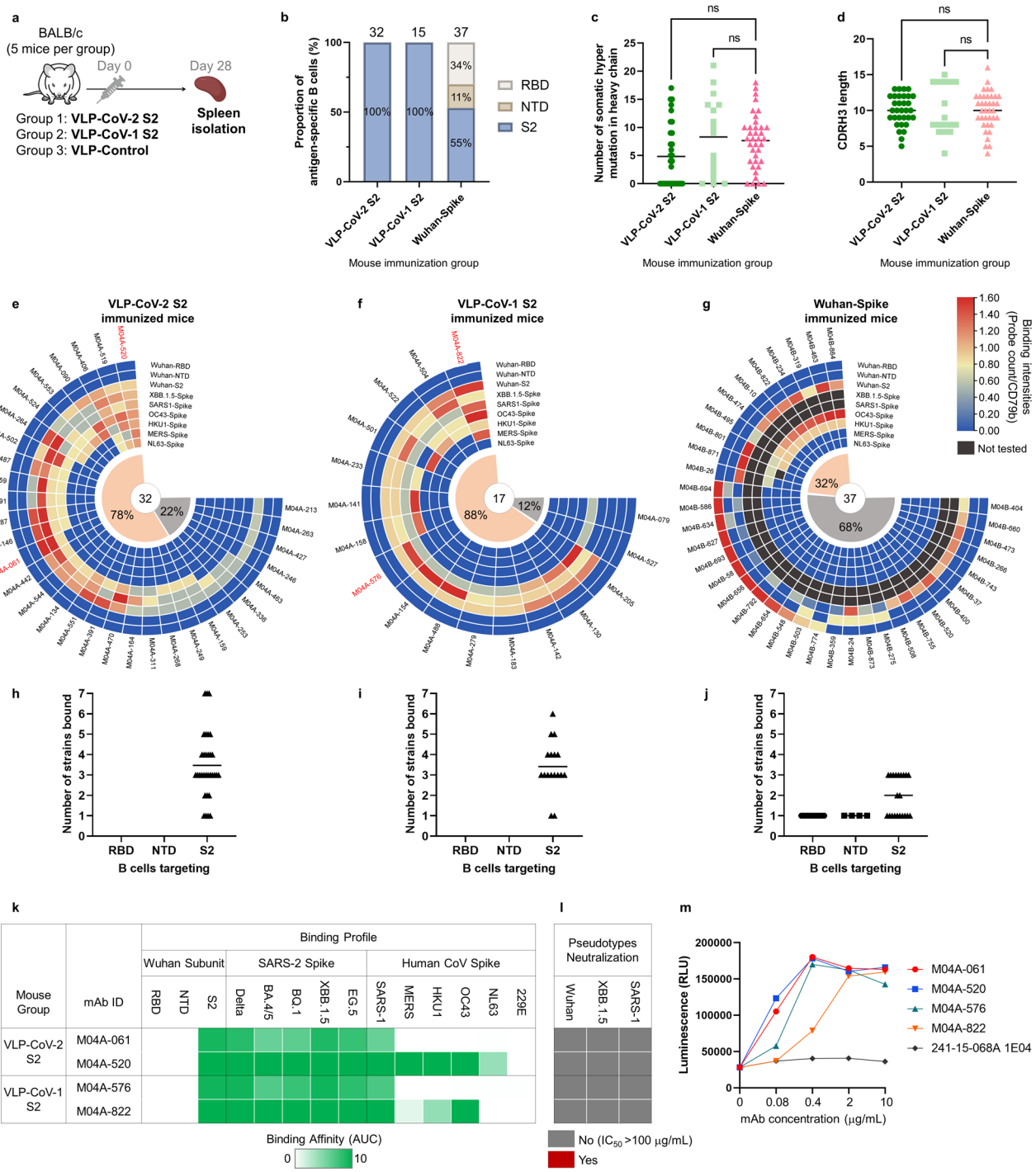

Fig. 5 | Characterization of S2 vaccine-induced B cells and mAbs. a Schema of mice immunization. S2 VLP or control VLP (7.5 μg/mouse) combined with the AS03 adjuvant and Poly(I:C) were injected subcutaneously into BALB/c mice ($n = 5$ per group, 10–12 weeks old). Spleen samples were collected four weeks after immunization. Created in BioRender. Wilson, P. (2024) https://BioRender.com/a30b566. **b** Proportion of B cells binding to indicated subunit probes in each immunization group. The numbers of B cells analyzed are shown above each bar. **c** Number of somatic hypermutations or (**d**) complementarity determining region 3 (CDR3) amino acid length in the IGHV in each immunization group. Significance was assessed by one-way ANOVA followed by Dunnett's test. **e**–**g** Probe binding profile of B cells against Wuhan-subunits or Human CoV spikes. Binding intensities are obtained by dividing the probe count by the CD79b count. The numbers in the center of the pie graphs indicate the number of B cells analyzed. The pink pie chart shows B cells that cross-reacted with SARS-CoV-2 and Human CoV, and the gray pie chart shows B cells that are specifically bound to either. **h**–**j** Number of strains bound by B-cell clones in mice immunized with VLP-CoV-2 S2, VLP-CoV-1 S2, and Wuhan Spike, respectively. 32 B cells were analyzed for 5h, 17 B cells for 5i, and 37 B cells for 5j. **k** Binding specificity of mAbs generated from S2 VLP immunized mice against Wuhan subunits, SARS-CoV-2 spikes, or Human CoV spikes. Binding data are represented as areas under the curve (AUC). **l** IC50 of the neutralization potencies of mAbs against SARS-CoV-2 spike pseudotyped viruses. **m** Activation of the ADCC signaling pathways. FcγR-mediated signaling activation in effector cells expressing human FcγRIIIa was induced by co-culture with Spike-expressing CHO cells. Signaling activation was measured in two technically independent experiments. The mAb clone 241-15-068 A 1E04 (anti-HA mAb) was used as a negative control. RLU, relative light unit.

https://doi.org/10.1038/s41467-025-55824-y

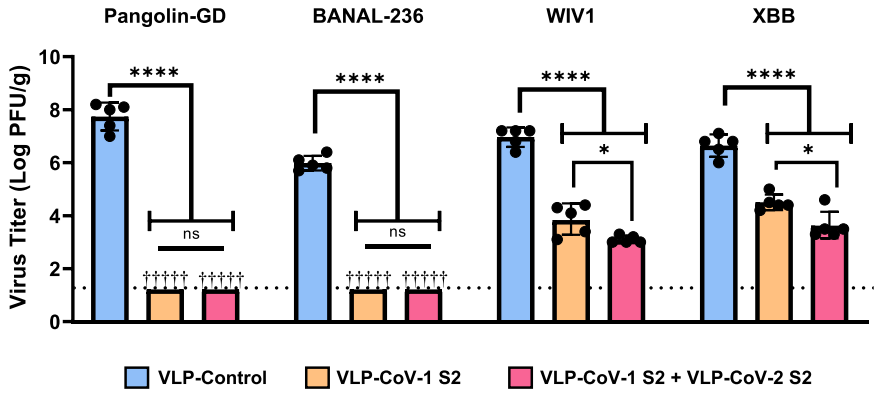

Fig. 6 | Protective efficacy of VLP-S2 after prime-boost. Virus titers in the lungs of K18-hACE2 mice immunized with two doses of S2 VLPs three days after infection with Pangolin-GD, BANAL-236, WIV1, and XBB (mean ± SD, $n = 5$ biological replicates). *$P < 0.05$ (WIV1 challenge group VLP-CoV-1 S2 vs VLP-CoV-1 S2 + VLP-CoV-2 S2: $P = 0.0220$; XBB.1 challenge group VLP-CoV-1 S2 vs VLP-CoV-1 S2 + VLP-CoV-2 S2: $P = 0.0218$), ****$P < 0.0001$. Significance was determined by an ordinary one-way ANOVA and Tukey post hoc multiple comparisons between groups for XBB and WIV1, and by Brown-Forsythe and Welch ANOVA and Games-Howell's multiple comparisons between groups for BANAL-236 and Pangolin-GD. ● or † indicate data from individual mice. † - No infectious virus was detected in the lungs of immunized mice. The detection limit (dotted line) = 1.3 $\log_{10}$ pfu/g.

Discussion

While we and others have previously shown that SARS-CoV-2 S2 subunit vaccines provide protection against SARS-CoV-2 and its variants, clade 1A sarbecovirus S2 antigens have not been evaluated against challenges with either clade 1A or clade 1B sarbecoviruses. While SARS-CoV-1 S2 subunit vaccines have been previously reported[32–34], their characterization was limited to T-cell and antibody responses. Here, we developed vaccines multivalently displaying stabilized SARS-CoV-1 and bat-CoV RsSHC014 S2 subunits on VLPs and showed they, along with VLPs presenting our previous $S2_{mutS2'}$ construct, significantly reduced virus titers in immunized mice challenged with MA10 (Fig. 3a). These results highlight the conserved nature of the S2 subunit, as clade 1A S2 antigens were able to protect against a clade 1B sarbecovirus challenge.

While vaccinations using solely S2-based vaccines have been evaluated against SARS-CoV-2 variants[14–20] and mouse-adapted SARS-CoV-1[19], challenges against related animal coronaviruses have not been reported except for a challenge against a clade 1B pangolin sarbecovirus in our previous work[14]. Given that the zoonotic spillover of a clade 1 sarbecovirus led to the SARS-CoV-1 2003 outbreak and the impact of the recent COVID-19 pandemic caused by another clade 1 sarbecovirus, it is paramount to determine the extent of protection provided by S2-based vaccines against clade 1 animal sarbecoviruses. Here, we showed that mice immunized with our CoV-1 S2 and CoV-2 S2 vaccines showed significantly reduced virus titers in the lungs after a single dose when challenged with WIV1 and RsSHC014, clade 1A sarbecoviruses that have been identified as having pandemic potential and poised for human emergence[5,6]. Both vaccines also fully protected against BANAL-236, and partially protected against Pangolin-GD after a single dose, two clade 1B animal sarbecoviruses.

While our S2 VLP vaccines significantly reduced virus titers in immunized mice challenged with the above-mentioned sarbecoviruses, the degree of protection was not the same for all groups. VLP-CoV-1 S2 reduced titers against clade 1A viruses to a greater extent than VLP-CoV-2 S2. The VLP-CoV-2 S2 result is similar to the results of Hsieh et al., who found that mice immunized with their SARS-CoV-2 S2-based vaccine were completely protected against MA10 challenge (Clade 1B) after two doses, but only partially protected against a mouse-adapted SARS-CoV-1 challenge (Clade 1A), even after repeating the challenge with mice immunized with three doses of their vaccine[19].

Tan et al. had previously reported that patients vaccinated against SARS-CoV-2 who were previously infected with SARS-CoV-1 had sera that showed more broad neutralization against both clade 1A and clade 1B sarbecoviruses compared to sera from vaccinated patients not previously infected[35]. Taking this result into account, while also considering the success of non-S2 based mixture vaccines in providing broad protection against sarbecoviruses[9,11,12], we decided to evaluate an S2 vaccine that included both CoV-1 and CoV-2 S2 antigens in our challenge models. We hypothesized that a VLP-S2 vaccine containing both CoV-1 S2 and CoV-2 S2 subunits would be more effective in providing protection against a broader range of sarbecoviruses compared to single-antigen vaccines despite the high homology in protein sequences between the CoV-1 S2 and CoV-2 S2. While two doses of VLP-CoV-1 S2 and the cocktail vaccine containing both S2 antigens conferred full protection against Pangolin-GD and BANAL-236, mice immunized with both S2 antigens showed significantly lower virus titers in the lungs when challenged with WIV1 and XBB compared to mice immunized with just the VLP-CoV-1 S2 (Fig. 6).

We showed that protection is elicited by our vaccines against MA10 despite very low neutralization titers against an early SARS-CoV-2 isolate elicited in C57BL/6 mice given two doses of the same vaccines (Supplementary Fig. 1). While we previously showed a modest neutralizing antibody response elicited by VLP-CoV-2 S2 in BALB/c mice, the dissimilarity found in this study could be attributed to the lower dose used for vaccinations (7.5 μg vs 14 μg) and the immunological differences in the mouse models (C57BL/6 vs BALB/c)[36,37]. To probe the mechanistic basis of this S2-based protection, we probed a possible role for cytotoxic T-cell responses. We found that mice treated with an anti-CD8 depletion antibody and immunized with VLP-CoV-1 S2 had similar virus titers in the lungs compared to non-T cell-depleted mice after MA10 challenge, suggesting $CD8^+$ effector T cells do not play a vital role in S2-based protection (Fig. 4b). Due to the high antibody endpoint titers against clade 1 S proteins seen in single-dose immunized mice (Fig. 3b), we hypothesized protection provided by our vaccines was likely a result of S2 non-neutralizing antibodies, which have been shown to confer protection against sarbecoviruses via effector functions[38–40]. The degree to which effector functions play a role in the protection provided by S2-based vaccinations has yet to be explored. Here, we found that VLP-CoV-1 S2-immunized wild-type mice challenged with MA10 had lower virus titers in the lungs compared to similarly immunized FcγR-deficient mice, supporting the view that S2-based protection is likely reliant on effector functions. Consistent with these results, monoclonal antibodies generated from VLP-S2-immunized mice activated ADCC signaling pathways in effector cells co-cultured with SARS-CoV-2 spike-expressing cells (Fig. 5m). Also consistent with endpoint titer (Fig. 3b) and neutralization data

(Supplementary Fig. 1), monoclonal antibodies generated from immunized mice were broadly binding but non-neutralizing (Fig. 5k, l).

Overall, we showed that our VLP-S2 vaccine constructs significantly reduced virus titers in the lungs in immunized mice challenged with XBB, Pangolin-GD, BANAL-236, WIV1, and RsSHC014. Although our vaccines significantly reduced virus titers in the lungs in mice challenged against XBB and WIV1, they did not reduce titers to undetectable levels. Further optimization of the vaccine regimen by increasing the number of doses or using different adjuvants may help further enhance the protective efficacy. Further optimization of the stability and structure of the S2-based antigens may also help boost the neutralizing antibody response. Our future efforts will focus on further expanding the breadth of protection of S2-based vaccines to sarbecoviruses from clades 2-4. The design of such pan-sarbecovirus S2-based vaccines may benefit from the incorporation of S2 antigens from these other clades.

It will also be important to further explore the impact of stabilization of S2-based antigens on their protective efficacy. In a recent study, Hsieh et al.[19] designed S2 constructs with inter-protomer disulfide bonds to attempt to lock the S2 subunit in a prefusion state. Even in the presence of these disulfide bonds, the apex still sampled a continuum of conformations between open and closed states. Importantly, immunization with our S2-based constructs protected female K18-hACE2 mice with challenges from a wide range of sarbecoviruses including XBB, WIV1, BANAL-236, and a pangolin sarbecovirus. Sera from immunized mice recognized full S proteins from a range of sarbecoviruses (Fig. 3b), confirming the ability of the elicited antibodies to recognize S2 domains in a prefusion conformation. B cells from immunized mice showed binding to a wide range of human CoV-derived S proteins (Fig. 5e, f). Sera from immunized mice showed efficacy in an ADCC assay (Supplementary Fig. 4c). Finally, while neutralization was not the most significant contributor to protection against viral challenge, we did see evidence of the elicitation of neutralizing antibodies (Supplementary Fig 1). While a potent neutralizing antibody response is not required for protection, further optimization of the stability and structure of the S2-based antigens may help boost this response.

Study limitations

This study used mouse models to evaluate the immune response elicited by our vaccines, the results of which may not translate directly in humans. While immune responses were consistent across mice in the same experimental group, a limitation of this study was the low number of mice used per group. In addition, the analysis of viral titers was only performed at 3 days post-infection. While this study evaluated our vaccines against many clade 1 sarbecoviruses, it didn't include all of them. Furthermore, no pre-existing immunity models were used in evaluating our vaccines in this study. As most people in the world have been either exposed to SARS-CoV-2 infection or been vaccinated at this point, their immune responses to S2-based vaccines, particularly clade 1A S2 vaccines, may be different compared to those of naïve mice evaluated here. Accordingly, this study primarily serves to further assess the extent of protection provided by S2-based vaccines.

Methods

Approval of animal studies

Immunization and challenge studies at the University of Wisconsin-Madison were performed under an approved protocol (Protocol Number: V006426) reviewed by the Institutional Animal Care and Use Committee. To minimize pain, virus infections were performed under isoflurane anesthesia. Mouse immunizations for B cell characterization were performed with the approval of the Weill Cornell Medical College Institutional Animal Care and Use Committee (Protocol Number: 2021-0024). Studies at the St. Jude Children's Research Hospital to validate T-cell depletion were performed with the approval of the Institutional Animal Care and Use Committee (Protocol Number: 098-100504).

Expression of S2 proteins

Six proline mutations were introduced in DNA encoding the S2 subunit regions of SARS-CoV-2 (YP_009724390.1, residues 686-1208), RsSHC014 (AGZ48806.1, residues 669–1191), and SARS-CoV-1 (P59594, residues 668–1190) based on the SARS-COV-2 HexaPro spike protein[26]. Additional mutations were made to residues to eliminate the S2′ protease cut site of the SARS-CoV-2 (K814G and R815G)[14], RsSHC014 (T796S, K797G, and R798G), and SARS-CoV-1 (T792S, K793G, and R794G) S2 regions. Each of these DNA segments was cloned into pcDNA3.1 (-) with the addition of an N-terminal mouse Ig Kappa signal peptide, C-terminal T4 fibritin trimerization domain, AviTag, and his-tag between the NcoI and XhoI restriction sites by Gene Universal, Inc. (Newark, DE). These three plasmids were transfected into Expi293F cells (RRID: CVCL_D615) per manufacturer protocol using the ExpiFectamine Transfection Kit (Thermo Fisher Scientific). Cultures were centrifuged at 6000 × *g* for 10 min 5 days post-transfection. The supernatant was collected and dialyzed into PBS for 2 h, after which it was dialyzed in fresh 1X PBS for an additional 2 h. The supernatant was then mixed with 1 mL of HisPure Ni-NTA resin (Thermo Fisher Scientific) and incubated overnight on a stir plate. The supernatant resin mixture was then loaded into a gravity flow column (G-Biosciences). After the column was washed with 90 mL of binding buffer (150 mM Tris, 150 mM NaCl, 20 mM Imidazole, pH 8), the resin was incubated for 5 min with 3 mL of elution buffer (150 mM Tris, 150 mM NaCl, 400 mM Imidazole, pH 8). Eluate was collected after the incubation period, and the elution process was repeated two more times resulting in a total volume of 9 mL. A 10 kDa MWCO spin filter (Millipore Sigma) was used to concentrate down the eluate, which was then further purified using a Superdex 200 Increase 10/30 column in PBS[12,14,25]. Protein concentration was quantified using the bicinchoninic acid assay (BCA) assay (Thermo Scientific).

Expression and purification of MS2

DNA encoding a single chain dimer of the MS2 coat protein was cloned into pET-28b between the NdeI and XhoI restriction sites by GenScript Biotech Corporation (Piscataway, NJ) with the additional insertion of an AviTag between the 14th and 15th residues of the first coat protein monomer[2,12,14,24]. This plasmid was co-transformed with a BirA-biotin-protein ligase expressing plasmid into BL21(DE3) competent E. coli (New England Biolabs) per manufacturer protocol. A 5 mL 2xYT media starter culture was made using the transformed *E. coli*, which were incubated at 37 °C overnight in a rotating incubator.[12,14,24,25]The starter culture was then added to 1 L of 2xYT and further grown at 37 °C in a shaking incubator at 225 rpm until it reached an optical density of 0.6 – 0.8, after which the culture was induced by adding 1 mL of of 1 M IPTG (Fisher BioReagents). Simultaneously, 50 mM D-biotin was added to the culture, and the incubation temperature was reduced to 30 °C.[12,14,24,25]The culture was centrifuged at 7000 × *g* for 7 mins after overnight incubation. The cell pellet was resuspended in 25 mL of lysis buffer (20 mM Tris base, 0.5 mg/mL lysozyme, 125 units of EMD Millipore benzonase, a quarter of a SigmaFast EDTA-free protease inhibitor cocktail tablet, pH 8) and incubated at 4 °C on a rocker for 20 min. Sodium deoxycholate (Alfa Aesar) was then added to the lysate to reach a final concentration of 0.1% (w/v). The lysate was sonicated on ice at 35% amplitude with 3-second pulses for 3 mins (Sonifier S-450, Branson Ultrasonics)[12,14,24,25]. The lysate was sonicated again after being allowed to rest on ice for 5 minutes. The lysate was centrifuged at 19,000 × *g* for 30 mins, the supernatant was collected and centrifuged again. The supernatant was collected a second time and diluted with 20 mM Tris Base, pH 8 to reach a total volume of 100 mL[12,14,24,25]. The supernatant was loaded onto four HiScreen Capto Core columns (Cytvia) in series using an ÄKTA Start system. The columns were

washed with 5 column volumes (CVs) of 20 mM Tris Base, pH 8 to elute out the MS2 protein. Collected MS2 fractions were combined and concentrated down using a 10 kDa MWCO spin filter (Millipore Sigma) before being further purified using a Superdex 200 Increase 10/30 column in 20 mM Tris, 20 mM NaCl, pH 8[12,14,24,25]. Protein concentration was quantified using the BCA assay (Thermo Scientific).

In vitro biotinylation of AviTagged MS2 and S2 proteins

The S2 and MS2 proteins were biotinylated using a BirA biotin-protein ligase standard reaction kit (Avidity LLC). A mixture of Biomix B (ATP, biotin, magnesium acetate) and BirA were added to the protein solutions, which were then mixed overnight at 4 °C. The following day, the protein-BirA solution was further supplemented with Biomix B and mixed at 37 °C for 2 h. After 2 h, additional Biomix B was added to the solution and left to mix overnight at 4 °C. The biotinylated proteins were then purified using a Superdex 200 Increase 10/30 column in 1X PBS to remove the excess BirA and biotin. The final protein concentration was quantified using the BCA assay (Thermo Scientific)[12,14,25].

Expression, refolding, and purification of streptavidin

SA encoding plasmid (Addgene plasmid #46367, a gift from Mark Howarth), was transformed into BL21(DE3) cells (New England Biolabs) per manufacturer protocol. The following protocol describes SA expression, refolding, and purification on a 2 L scale. Two 5 mL 2xYT starter cultures were made using the transformed BL21(DE3) cells[12,14,24,25,41,42]. The cultures were grown overnight in a 37 °C rotation incubator. The next morning, each starter culture was added to 1 L of 2xYT media and grown further on a shaking incubator until the OD reached 0.6 – 1.0, after which the cultures were induced by the addition of 1 mL of 1 M IPTG (Fisher BioReagents)[12,14,24,25,41,42]. The temperature was reduced to 30 °C, and the cultures were incubated overnight. The next day, the cultures were combined and centrifuged at 7000 × *g* for 7 mins. The resulting cell pellet was resuspended with 50 mL of resuspension buffer (50 mM Tris, 100 mM NaCl, pH 8.0) supplemented with 1 mg/mL lysozyme (Alfa Aesar) and 500 units of benzonase (EMD Millipore)[12,14,24,25,41,42]. The lysate was incubated on a rocker at 4 °C for 1 hour and homogenized for 30 s. Sodium deoxycholate (Alfa Aesar) was then added to the lysate to reach a final concentration of 0.1% (w/v), after which the lysate was sonicated at 35% amplitude for 3 min with 3-second pulses. The sonicated lysate was then centrifuged at 27000 × *g* for 15 min[12,14,24,25,41,42]. The supernatant was discarded, and the above-mentioned lysis process was repeated, except benzonase was excluded in the lysis buffer and the 4 °C incubation period was reduced to 30 min. Following the second centrifugation, the pellet was resuspended in 50 mL of wash buffer #1 (50 mM Tris, 100 mM NaCl, 100 mM EDTA, 0.5% (v/v) Triton X-100, pH 8.0), homogenized for 30 seconds, and then sonicated for 30 s at 35% amplitude. The lysate was centrifuged at 27,000 × *g* for 15 min, and this wash process was repeated two more times[12,14,24,25,41,42]. The pellet was then washed with a second wash buffer (50 mM Tris, 10 mM EDTA, pH 8.0), homogenized for 30 s, sonicated for 30 s at 35% amplitude, and centrifuged at 15,000 × *g* for 15 min. This wash process was repeated one more time. The pellet was then resuspended in 10 mL of resuspension buffer[12,14,24,25,41,42]. Guanidine hydrochloride was added to the mixture to reach a final concentration of 7.12 M and then mixed at room temperature for 1 h. The mixture was then centrifuged at 12,000 × *g* for 12 min, transferred to a syringe, loaded onto a syringe pump, and allowed to drip at a rate of 30 mL/hour into 1 L of chilled, rapidly stirring PBS. The solution was mixed overnight at 4 °C then centrifuged the next day at 17000 × *g* for 15 min to remove insoluble protein[12,14,24,25,41,42]. The supernatant was then filtered through a 0.45 µm bottle-top filter. Ammonium sulfate was slowly added to the filtrate while it was rapidly stirring to a final concentration of 1.9 M. The solution was mixed further for 3 h at 4 °C, centrifuged again at 17000 × *g* for 15 min, then filtered again[12,14,24,25,41,42]. More ammonium sulfate was added to the filtrate while it was stirring vigorously to a final concentration of 3.68 M. The mixture was stirred overnight at 4 °C, and the SA was pelleted out by centrifuging it at 17000 × *g* for 15 minutes. The SA pellet was resuspended using 20 mL of Iminobiotin Affinity Chromatography (IBAC) binding buffer (50 mM Sodium Borate, 300 mM NaCl, pH 11.0). Afterward, 5 mL of Pierce Iminobiotin Agarose (Thermo Scientific) was added to a gravity flow column (G-Biosciences) and then equilibrated with 25 mL of IBAC binding buffer[12,14,24,25,41,42]. The resuspended SA was loaded onto the column and then washed with 50 mL of IBAC binding buffer. The SA was eluted with 20 mL of IBAC elution buffer (20 mM Potassium Phosphate, pH 2.2) and dialyzed in PBS overnight. The SA was then concentrated using a 10 kDa MWCO centrifugal filter (Millipore Sigma), and the concentration was measured by absorbance at 280 nm[12,14,24,25,41,42].

Assembly and purification of MS2-SA VLPs

A concentrated solution of 20x molar excess of SA (at a minimum concentration of 30 mg/mL) was stirred rapidly in a small glass vial. Biotinylated MS2 (at a maximum concentration of 700 µg/mL) was added in 2.5 µL increments to the SA. The MS2-SA mixture was then loaded onto a Superdex 200 Increase 10/30 column in PBS to separate the MS2-SA VLPs and excess SA. The MSA-SA samples were quantified via SDS polyacrylamide gel electrophoresis (SDS-PAGE). The MS2-SA samples were mixed with Nu-PAGE lithium dodecyl sulfate (LDS) sample buffer (Invitrogen) and then heated for 30 min at 90 °C. Afterward, the MS2-SA samples were loaded onto a polyacrylamide gel with SA standard samples of known concentrations. The SA band intensities of the MS2-SA samples were compared to the band intensities of the SA standard samples to determine the SA concentration of the MS2-SA samples[12,14,24,25].

Preparation of VLP-S2

The optimal ratio of biotinylated S2 to MS2-SA was determined using analytical SEC. Mixtures of 8 µg of the S2 antigens and varying amounts of MS2-SA were loaded onto a Superdex 200 increase 10/300 SEC column (Cytiva). The optimal ratio was determined to be the ratio that included the least amount of MS2-SA in the mixture and also resulted in a chromatogram without a peak corresponding to excess S2 antigen[12,14,24,25].

SDS-PAGE

Protein samples were deglycosylated with PNGase F (New England BioLabs), then diluted with 2 µL of 2-Mercaptoethanol and 5 µL of Nu-PAGE lithium dodecyl sulfate (LDS) sample buffer (Invitrogen). Samples were heated at 98 °C for 30 min then loaded alongside a PageRuler Plus Prestained Protein Ladder (Thermo Scientific) into a 4–12% Bis-Tris gel (Invitrogen). The gel was run at 120 V for 50 minutes in an MES-SDS buffer. The gels were imaged with ChemiDoc MP imaging system and Image Lab 5.2.1 software (Bio-Rad) after being stained with Imperial Protein Stain (Thermo Scientific) for 30 min and destained overnight[14].

Expression of S2P6 antibody

The heavy and light chains of the S2P6 antibody[43] were cloned into TGEX-HC and TGEX-LC vectors (Antibody Design Labs), respectively, and expressed in Expi293F cells using the ExpiFectamine Transfection Kit (Thermo Fisher Scientific). After a 6-day 37 °C incubation, cells were centrifuged at 6000 × g for 15 min, and the supernatant was diluted in MabSelect Binding Buffer (20 mM sodium phosphate, 150 mM NaCl, pH 7.2). The diluted supernatant was then injected onto a 1-mL MabSelect SuRe column (Cytiva) connected to an ÄKTA Start to purify the protein. The protein was then further purified by SEC. Fractions with the protein were collected and dialyzed into PBS, and the protein concentration was determined using the BCA assay. Transfection and MabSelect purification were done according to manufacturer instructions.

S2 and VLP-S2 ELISA

Protein samples were diluted in PBS to a concentration of 1 μg of S2 per 1 mL. For each well of a Nunc Maxisorp 96-well plate, 100 μL of diluted protein solution was added (total 0.1 μg of S2 per well) and incubated for 1 hour. The protein solution was removed from the plate, which was then blocked with 200 μL of a 5% BSA (EMD Millipore) in PBST (0.05% Tween 20) and allowed to incubate for another hour. Afterward, the BSA solution was discarded, and the wells were washed three times with 100 μL of PBST. A stock solution of the primary S2P6 antibody (at 1.9 mg/mL) was diluted 1:30000 in 1% BSA in PBST, and 100 μL of this solution was added to the wells. After 1 hr, the solution was removed, and the plate was washed again three times with PBST, after which 100 μL of horseradish peroxidase-conjugated anti-human IgG Fc goat antibody (MP Biomedical, catalog #674171) diluted 1:5000 in 1% BSA in PBST was added to the wells[12,14,24,25]. After incubating for an hour, the solution was removed, and the plates were washed again three times with PBST. 100 μL of TMB (Thermo Scientific) was added to each well, and after 3 min, 160 mM sulfuric acid was added to stop development. The plates were read using a Synergy H4 plate reader (BioTek) with Gen5 2.07 software (BioTek) at 450 nm[12,14,24,25].

Dynamic light scattering

Measurements were taken using a Zetasizer Nano (Malvern). S2 and VLP-S2 proteins were diluted so there was 5 μg of S2 per 100 μL of PBS, and MS2-SA was diluted so there was approximately 2 μg in 100 μL. 100 μL of diluted protein solution was added to a UVette (Eppendorf), and 13 acquisitions per sample were collected at 25 °C. Results were displayed as % volume.

Analytical SEC

S2 and VLP-S2 proteins were diluted so there was 8 μg of S2 per 950 μL of PBS. They were loaded into a Superdex 200 Increase 10/300 Column (Cytiva) using an ÄKTA Pure and the Unicorn 7 control system (Cytiva). They were eluted with a full column volume of PBS flowing at 0.65 mL/min, while the absorbance was monitored at 210 nm.

Amino acid Identity and phylogenetic trees

All spike amino acid sequences were retrieved from GenBank. Clustal Omega 1.2.3 (Conway Institute, UCD Dublin) was used to align sequences. These alignments were used to calculate the percent identity of amino acids for each paired comparison. PhyML 3.3.20220408 (Stephane Guindon, University of Montpellier) was used to generate the Maximum likelihood phylogenetic trees. This program used the LG amino acid substitution model and a maximum parsimony starting tree. TreeViewer 2.0.1 (Giorgio Bianchini, University of Bristol) was used to visualize the phylogenetic trees.

Negative-stain transmission electron microscopy

For negative-stain transmission electron microscopy (NS-TEM) on VLP-S2 variants, 4 μL of the diluted samples were applied onto glow-discharged 200-mesh copper grids (CF200-Cu; Electron Microscopy Sciences, PA). The grids were washed with drops of distilled water (3X), drops of staining solution of 1% phosphotungstic acid (PTA, pH 6 ~ 7) (2X), followed by 1 min of staining drop incubation. Excess stain was removed from the grids with backside blotting with filter paper, the grids were then allowed to air-dry. The grids were imaged with a low dose of 50 ~ 60 e-/Å2, under a nominal magnification of 73 kx (pixel size of 2.0 Å), defocus of − 0.5 to − 2 μm, on a Talos L120C transmission electron microscope (TEM, ThermoFisher Scientific, Hillsboro, OR), operating at 120 kV. Images were captured on a 4 K x 4 K Ceta CMOS camera (ThermoFisher Scientific, Hillsboro, OR) using the SerialEM 3.8[44] software package.

Biosafety and containment for coronaviruses

Research with sarbecoviruses was performed under biosafety level 3 agriculture (BSL-3 AG) containment at the Influenza Research Institute with an approved protocol reviewed by the University of Wisconsin-Madison's Institutional Biosafety Committee. The laboratory is designed to meet and exceed the standards outlined in Biosafety in Microbiological and Biomedical Laboratories (6th edition).

Cell lines and viruses

All virus stocks were propagated on Vero E6 TMPRSS2 cells (National Institute of Infectious Diseases, Japan) which were maintained in high glucose Dulbecco's modified Eagle's medium (DMEM) containing 10% fetal bovine serum (FBS) and antibiotic/antimycotic solution along with G418 (1 mg/mL). For consistency, virus titrations of tissue samples were performed on Vero E6 TMPRSS2-T2A-ACE2 cells (NIAID Vaccine Research Center; Dr. Barney Graham). This cell line was maintained in DMEM supplemented with 10% FBS, 10 mM HEPES (pH 7.3), and antibiotic/antimycotic solution along with puromycin (10 μg/mL). Both cells are tested monthly for mycoplasma contamination by PCR and are confirmed to be mycoplasma-free.

In the mouse challenge studies, the following viruses were used, SARS-CoV-2 mouse-adapted strain (MA10 variant, GenBank: MT952602.1), XBB (hCoV-19/Japan/TY41-795/2022 (Accession ID: EPI_ISL_16355653), Banal-20-236/Laos/2020 (GenBank: MZ937003), WIV1 (GenBank: KF367457), RsSHC014 (GenBank: KC881005), and BetaCoV/pangolin/Guandong/1/2019 (Accession ID: EPI_ISL_410721). For the live virus neutralization assay, the early isolate SARS-CoV-2/UT-HP095-1N/Human/2020/Tokyo (HP095) was used (GenBank: PQ571724)[45].

Mouse immunizations and challenge studies

C57BL/6, K18-hACE2, and BALB/c mice were purchased from Jackson Laboratories while FcγR knockout mice, deficient in the γ chain subunit of the FcγRI, FcγRIII, and FcεRI receptors, and the wild-type BALB/c control mice were purchased from Taconic. All mice were females and at the age of 10–12 weeks at the start of the studies. Mice were acclimated to the ambient conditions of the facilities (25–28 °C and 35–45% humidity) prior to the start of experiments, allowed access to food and water ad libitum, kept on a 12 h on/off light cycle, and given enrichment. Mice were immunized by subcutaneous injection with a total volume of 250 μL of an equal mixture of VLP vaccine preparations (7.5 μg of each S2 antigen) and adjuvant mixture (AddaS03 with poly I:C [InvivoGen]). Additional mice were immunized with Pfizer's BNT162b2 mRNA virus at a dose of 1.0 μg by intramuscular inoculation. Under anesthesia (isoflurane), mice were infected intranasally with 10^5 plaque-forming units (pfu) of challenge virus in 30 μL of the total volume of the diluted virus. Animals were humanely sacrificed by an overdose of isoflurane three days after infection to collect lung tissue and nasal turbinate samples to measure the amount of virus.

Anti-CD8 antibody treatment

To deplete CD8 + T cells, mice were inoculated intraperitoneally with 500 μL of PBS with the anti-CD8 depleting antibody at a 1:10 dilution (Harlan Sprague-Dawley, clone 2.43, lot # 70088)[28]. Treatments started three days and one day prior to immunization (day − 3 and day − 1), on the day of immunization (day 0), and after immunization (day + 1, + 3, + 6, + 9 and + 12).

B cell characterization studies

The following B cell characterization studies were performed using cells isolated from mouse spleen samples that were collected four weeks after immunization.

Probe generation for B cell characterization

Subunit proteins (RBD, NTD, and S2) and HexaPro or 2 P spike proteins (SARS-CoV-2 XBB.1.5, SARS-CoV-1, MERS-CoV, OC43, HKU1, and NL63) were biotinylated for 30 min on room temperature using EZ-Link Sulfo-NHS-Biotin, No-Weigh Format (Thermo Fisher) according to the manufacturer's instructions. Unreacted biotin was removed by passage through a 7 K MWCO desalting column (Zeba spin, Thermo Fisher). Biotinylated proteins were then conjugated to Biolegend TotalSeq PE streptavidin (PE-SA), APC streptavidin (APC-SA) oligos at a 0.72:1 molar ratio of antigen to PE-SA or APC-SA. The amount of antigen was chosen based on a fixed amount of 0.5 µg PE-SA or APC-SA and diluted in a final volume of 10 µL. PE-SA or APC-SA was then added gradually to 10 µL biotinylated proteins 5 times on ice, 1 µL PE-SA or APC-SA (0.1 mg/mL stock) every 20 min for a total of 5 µL (0.5 µg). The reaction was then quenched with 5 µL 4 mM Pierce biotin (Thermo Fisher) for 30 min for a total probe volume of 20 µL. Probes were then used immediately for staining.

Single B cell sorting and 10X Genomics library preparations

For antigen-specific B cell sorting, B cells were enriched using EasySep Mouse Pan-B Cell Isolation Kit (STEMCELL). B cells were stained with anti-mouse B220 FITC (BioLegend), anti-mouse IgM PE-Cyanine7 (Thermo Fisher), anti-mouse IgD APC-Cyanine7 (BioLegend), and antigen probes (PE or APC) for 30 min on ice in 1 × phosphate-buffered saline (PBS) supplemented with 0.2% bovine serum albumin (BSA) and 2 mM Pierce biotin. Cells were subsequently washed with 1 × PBS with 0.2% BSA and resuspended at a maximum of 10 million cells/mL in 1 × PBS supplemented with 0.2% BSA and 2 mM Pierce biotin for downstream cell sorting using the Aurora CS Cell Sorter (Cytek Biosciences). BB220 + / IgM-/IgD-/antigen-PE-positive cells were sorted as probe positive.

Single-cell RNA-seq and B cell receptor sequencing

After sorting antigen-specific B cells, the cells were immediately processed to generate single-cell gel beads in emulsion (GEM) by loading them onto the 10X Chromium Controller. The cDNA was purified from each GEM, followed by the generation of 10X Genomic libraries, which included 5′ Gene Expression, V(D)J BCR, and ADT (Feature Barcoding). All purified libraries were pooled and sequenced using an Illumina NextSeq1000. Cell Ranger (version 7.1.0) was used to perform raw sequence processing, sample demultiplexing, barcode processing, single-cell 5′ transcript counting, and B cell receptor repertoire sequence assembly[46]. The reference genome assembly for the transcriptome is refdata-gex-mm10-2020-A, and the reference genome assembly for V(D)J is refdata-cellranger-vdj-GRCm38-alts-ensembl-7.0.0. The data obtained from Cell Ranger were subsequently used for downstream analysis using the Seurat toolkit (version 4.3.0) (an R package for transcriptome, cell surface protein, and antigen probe analyses) and IgBlast (version 1.15) for immunoglobulin gene analysis. Cell quality control (QC), normalization, data scaling, linear dimensional reduction, clustering, differential expression analysis, batch effect correction, and data visualization were performed using Seurat (version 4.3.0). QCs of cells were performed further to exclude cells with < 200 and > 2500 detected genes and cells expressing a high percentage of mitochondrial genes. Transcriptome RNA data were analyzed using conventional log normalization. We performed a principal component analysis (PCA) and used the top 20 principal components (PCs) for linear dimensional reduction and clustering. Only filtered, high-quality cells were clustered in this analysis using the Louvain algorithm implemented in Seurat under a resolution of 0.6 for clustering. Batch effects across different data sets were normalized using an Anchor method implemented in Seurat[46].

Monoclonal antibody production

Antibody heavy and light chain genes obtained by 10X Genomics V(D)J sequencing analysis were synthesized by Integrated DNA Technologies. The synthesized fragments for heavy and light chains with 5′ and 3′ Gibson overhangs were then cloned into human IgG1 and human kappa or lambda light chain expression vectors by Gibson assembly[47]. The heavy and light chains of the corresponding mAb were co-transfected into HEK293T cells. After 4 days, mAbs secreted into the medium supernatant were harvested and purified using protein A-agarose beads (Thermo Fisher).

Enzyme-linked immunosorbent assay (ELISA) for mAbs and mouse serum

High-protein-binding microtiter plates (Costar) were coated with 50 µl of subunit or spike proteins at 2 µg/mL in a 1 × PBS solution overnight at 4 °C. The plates were washed 3 times the next day with 1 × PBS supplemented with 0.05% Tween 20 and blocked with 200 µL of 1 × PBS containing 20% fetal bovine serum (FBS) for 1 h at 37 °C. mAbs were serially diluted 1:3 starting at 10 µg/mL while mouse sera were serially diluted 1:2 starting at 1:20; both were incubated for 1 h at 37 °C. The plates were then washed 3 times and incubated with horseradish peroxidase (HRP)-conjugated goat anti-human IgG antibody for mAbs or anti-mouse IgG antibody for mouse serum (Jackson ImmunoResearch) diluted 1:5000 for 1 h at 37 °C, and plates were subsequently developed with the Super AquaBlue enzyme-linked immunosorbent assay (ELISA) substrate (eBioscience) for 10 min. The absorbance was measured at 405 nm on a microplate spectrophotometer (Bio-Rad). All mAbs were tested in duplicate, and each experiment was performed twice, while mouse serum was tested in singlets from groups of four immunized mice.

Monoclonal antibody pseudovirus neutralization assay

Virus neutralization assays were performed with SARS-CoV-2 spike pseudotyped virus that generated with the recombinant replication-deficient vesicular stomatitis virus (VSV) containing luciferase instead of the VSV-glycoprotein (VSV-G) gene (Kerafast). Vero E6-ACE2-TMPRSS2 cells (BEI) were seeded in 96-well white, flat-bottom plates (Corning) at 40,000 cells/well in culture medium and cultured overnight at 37 °C with 5% CO2. Each mAb was four-fold serially diluted in culture medium from 100 µg/mL (100–0.39 µg/mL). mAb dilutions were mixed 1:1 with a certain amount (325–1300 TCID50/mL) of pseudovirus for 30 min at 37 °C prior to addition to Vero E6-ACE2-TMPRSS2 cell monolayers and incubation at 37 °C with 5% CO2 for 24 h. Supernatants were removed, and the cells were lysed with luciferase reagent (Promega). Luminescence was measured on a Spectramax M5 (Molecular Devices), and neutralization titers (IC50) were calculated using an Excel macro[48].

Antibody-dependent cellular cytotoxicity (ADCC) assay

ADCC reporter assays were performed using ADCC Reporter Bioassay kits (Promega) according to the manufacturer's instructions. The activation of ADCC signaling in effector cells were measured using CHO cells expressing the SARS-CoV-2 spike. Briefly, CHO cells were plated at a density of 10,000 cells/well in a flat-bottom white 96-well plate (Corning). The cells were used as target cells 24 hours later. The medium of the target cells was replaced with test mAb five-fold-diluted (10–0.08 µg/mL) or mouse serum five-fold-diluted (1/20–1/62500) in the assay buffer (Promega). The mAb clone 241-15-068 A 1E04 (anti-HA mAb) was used as a negative control[49]. ADCC bioassay effector cells (a Jurkat cell line stably expressing human FcγRIIIa, human CD3γ, and an NFAT-response element driving expression of a firefly luciferase) were added to the antibody-treated target cells and incubated for 6 h at 37 °C. The firefly luciferase activity was then measured using luciferase assay regents (Promega).

Competition biolayer interferometry (BLI)

The competition among S2 mAbs was determined through a pairwise competition conducted using biolayer interferometry (BLI) with an

Octet K2 instrument (ForteBio/Sartorius). The SARS-CoV-2 Wuhan S2 monomer antigen was biotinylated with (EZ-Link Sulfo-NHS-Biotin, ThermoFisher), desalted, and loaded at a concentration of 250 nM onto streptavidin biosensor (Forte Bio/Sartorius) for 150 s. After the sensor was soaked in kinetic buffer (PBS) for 30 s, the sensor was captured with the first mAb as an association step for 300 s, followed by the second mAb for another 300 s. The response units were collected from Octet Data Analysis HT software (Forte Bio/Sartorious). The competition percentage was calculated by subtracting the ratio of the binding response of the secondary mAb in the presence of the first mAb to the binding response of the first mAbs alone from 1, and then multiplying the result by 100. Antibodies with > 50% competition was considered as competing.

Statistics and reproducibility

SDS-PAGE gel of S2 and S2-VLP samples (Fig. 2b) was run twice using different preparations of each sample with similar results. At least 80 images were collected for TEM imaging (Fig. 2d) and analyzed from one S2-VLP preparation per sample with similar results. The binding characterization of S2P6 by ELISA (Fig. 2e) was conducted once in triplicate for each condition, presented as mean ± SD. Group sizes were determined based on previous S2-antigen vaccine studies, and no sample-size calculations were performed prior to the study in order to determine the power of these studies. Animal groups were not blinded to the researchers. Endpoint titers (Fig. 3b) were determined by conducting a single assay using sera from each mouse ($n = 4$). The data is presented as geometric mean ± geometric SD, significance was determined by Brown-Forsythe and Welch ANOVA and Games-Howell's multiple comparisons between groups for SARS-CoV-2, Pangolin-GD, SARS-CoV-1, and RsSHC014 S proteins, and by ordinary one-way ANOVA and Tukey post hoc multiple comparisons between groups for Rc-o319 and WIV1 S proteins. Virus titers in the lungs of VLP-S2 immunized mice challenged with MA10, XBB, Pangolin-GD, BANAL-236, WIV1, and RsSHC014 (Fig. 3a–c) were presented as mean ± SD ($n = 4$ for all groups). The significance was determined by an ordinary one-way analysis of variance (ANOVA) and Tukey's multiple comparisons between groups ($\alpha = 0.05$) for MA10, XBB, Pangolin-GD, and RsSHC014 lung titers and by Brown-Forsythe and Welch ANOVA and Games-Howell's multiple comparisons between groups ($\alpha = 0.05$) for BANAL-236 and WIV1 lung titers. Lung titers for Pfizer-BioNTech bivalent vaccine immunized mice challenged with WIV1 (Fig. 3d) were presented as mean ± SD ($n = 4$ for all groups). Significance was determined by two-tailed Welch's t test. For the T-cell depletion study (Fig. 4a), virus titers in the lungs of immunized mice were presented as mean ± SD (mean ± SD, $n = 5$ for VLP-control and S2 CD8(+) groups, $n = 4$ for S2 CD8(-) group). The significance was determined by an ordinary one-way ANOVA and Tukey's multiple comparisons between groups ($\alpha = 0.05$). For the FcgR KO mice study (Fig. 4b), virus titers in the lungs of immunized mice were presented as mean ± SD ($n = 5$ for wild-type BALB/c mice and $n = 4$ for FcR KO mice). The significance for somatic hypermutations and complementarity determining region 3 (CDR3) amino acid length in the IGHV (Fig. 5c, d) was determined by ordinary one-way ANOVA and Dunnett's test. Significance was determined by two-tailed Welch's t test. Virus titers in the lungs of mice vaccinated with two doses of the VLP-S2s and challenged with XBB, Pangolin-GD, BANAL-236, and WIV1 (Fig. 6) were presented as mean ± SD ($n = 5$ for all groups). The significance was determined by an ordinary one-way analysis of variance (ANOVA) and Tukey's multiple comparisons between groups ($\alpha = 0.05$) for XBB and WIV1 lung titers and by Brown-Forsythe and Welch ANOVA and Games-Howell's multiple comparisons between groups ($\alpha = 0.05$) for BANAL-236 and Pangolin-GD lung titers. For tests of significance, assumptions of the normality of residuals and homogeneity of variance were validated by the D'Agostino-Pearson test and Brown–Forsythe test, respectively. All statistical analysis was carried out using Prism 9 (GraphPad).

Reporting summary

Further information on research design is available in the Nature Portfolio Reporting Summary linked to this article.

Data availability

Data supporting the conclusions of this paper can be found within the paper, Supplementary Information, and Source Data file. Protein sequences for MS2-AviTag and the S2 proteins are available in Supplementary Table 2. GenBank and RefSeq accession numbers for Fig. 1 are available in Supplementary Table 3. Structures used to generate Fig. 2a are available from the PDB using accession codes 2MS2, 3RY2, and 6VSB. Accession numbers correlating to viruses used are listed in the methods section of this paper: MT952602.1 [https://www.ncbi.nlm.nih.gov/nuccore/MT952602.1], EPI_ISL_16355653 [https://doi.org/10.1038/s42003-024-06015-w], MZ937003, KF367457, KC881005, PQ571724 [https://www.ncbi.nlm.nih.gov/nuccore/PQ571724], and EPI_ISL_410721 [https://gisaid.org]. Raw sequencing data have been deposited to the NCBI Gene Expression Omnibus (GEO) under accession number GSE282247. Unprocessed SDS-PAGE gel images for Fig. 2b are available in Supplementary Fig. 5 and Source Data file. Source data for Figs. 2c–e, 3, 4b, c, 5b–m,and 6 are available in the Source Data file. Source data are provided in this paper.

Code availability

VGenes, which was used for BCR sequencing analysis, is freely available from the Wilson Lab GitHub page at: https://github.com/WilsonImmunologyLab.

References

1. Huang, Y., Yang, C., Xu, X.-f, Xu, W. & Liu, S.-w Structural and functional properties of SARS-CoV-2 spike protein: potential antivirus drug development for COVID-19. *Acta Pharmacol. Sin.* **41**, 1141–1149 (2020).
2. Shah, P., Canziani, G. A., Carter, E. P. & Chaiken, I. The case for S2: The potential benefits of the S2 subunit of the SARS-CoV-2 spike protein as an immunogen in fighting the COVID-19 pandemic. *Front. Immunol.* **12**, 637651 (2021).
3. Amanat, F. et al. SARS-CoV-2 mRNA vaccination induces functionally diverse antibodies to NTD, RBD, and S2. *Cell* **184**, 3936–3948.e10 (2021).
4. Wang, L., Møhlenberg, M., Wang, P. & Zhou, H. Immune evasion of neutralizing antibodies by SARS-CoV-2 Omicron. *Cytokine Growth Factor Rev.* **70**, 13–25 (2023).
5. Menachery, V. D. et al. A SARS-like cluster of circulating bat coronaviruses shows potential for human emergence. *Nat. Med.* **21**, 1508–1513 (2015).
6. Menachery, V. D. et al. SARS-like WIV1-CoV poised for human emergence. *Proc. Natl. Acad. Sci. USA* **113**, 3048–3053 (2016).
7. LeDuc, J. W. & Barry, M. A. SARS, the First pandemic of the 21st century. *Emerg. Infect. Dis.* **10**, e26 (2004).
8. Cohen, A. A. et al. Mosaic RBD nanoparticles protect against challenge by diverse sarbecoviruses in animal models. *Science* **377**, eabq0839 (2022).
9. Cohen, A. A. et al. Mosaic nanoparticles elicit cross-reactive immune responses to zoonotic coronaviruses in mice. *Science* **371**, 735–741 (2021).
10. Lee, D. B. et al. Mosaic RBD nanoparticles induce intergenus cross-reactive antibodies and protect against SARS-CoV-2 challenge. *Proc. Natl. Acad. Sci.* **120**, e2208425120 (2023).
11. Brinkkemper, M. et al. Co-display of diverse spike proteins on nanoparticles broadens sarbecovirus neutralizing antibody responses. *iScience* **25**, 105649 (2022).
12. Halfmann, P. J. et al. Broad protection against clade 1 sarbecoviruses after a single immunization with cocktail spike-protein-nanoparticle vaccine. *Nat. Commun.* **15**, 1284 (2024).

13. Zhou, P. et al. Broadly neutralizing anti-S2 antibodies protect against all three human betacoronaviruses that cause deadly disease. *Immunity* **56**, 669–686 (2023).
14. Halfmann, P. J. et al. Multivalent S2-based vaccines provide broad protection against SARS-CoV-2 variants of concern and pangolin coronaviruses. *EBioMedicine* **86**, 104341 (2022).
15. Ng, K. W. et al. SARS-CoV-2 S2–targeted vaccination elicits broadly neutralizing antibodies. *Sci. Transl. Med.* **14**, eabn3715 (2022).
16. Pang, W. et al. A variant-proof SARS-CoV-2 vaccine targeting HR1 domain in S2 subunit of spike protein. *Cell Res.* **32**, 1068–1085 (2022).
17. Lu, Y. et al. HR121 targeting HR2 domain in S2 subunit of spike protein can serve as a broad-spectrum SARS-CoV-2 inhibitor via intranasal administration. *Acta Pharm. Sin. B* **13**, 3339–3351 (2023).
18. Kapingidza, A. B. et al. Engineered immunogens to elicit antibodies against conserved coronavirus epitopes. *Nat. Commun.* **14**, 7897 (2023).
19. Hsieh, C.-L. et al. Prefusion-stabilized SARS-CoV-2 S2-only antigen provides protection against SARS-CoV-2 challenge. *Nat. Commun.* **15**, 1553 (2024).
20. Lee, J. et al. A broadly generalizable stabilization strategy for sarbecovirus fusion machinery vaccines. *Nat. Commun.* **15**, 5496 (2024).
21. Starr, T. N. et al. ACE2 binding is an ancestral and evolvable trait of sarbecoviruses. *Nature* **603**, 913–918 (2022).
22. Seifert, S. N. et al. An ACE2-dependent Sarbecovirus in Russian bats is resistant to SARS-CoV-2 vaccines. *PLOS Pathog.* **18**, e1010828 (2022).
23. Castro, A., Carreño, J. M., Duehr, J., Krammer, F. & Kane, R. S. Refocusing the immune response to selected epitopes on a Zika virus protein antigen by nanopatterning. *Adv. Healthc. Mater.* **10**, 2002140 (2021).
24. Frey, S. J. et al. Nanovaccines displaying the influenza virus hemagglutinin in an inverted orientation Elicit an enhanced stalk-directed antibody response. *Adv. Healthc. Mater.* **12**, 2202729 (2023).
25. Chiba, S. et al. Multivalent nanoparticle-based vaccines protect hamsters against SARS-CoV-2 after a single immunization. *Commun. Biol.* **4**, 597 (2021).
26. Hsieh, C. L. et al. Structure-based design of prefusion-stabilized SARS-CoV-2 spikes. *Science* **369**, 1501–1505 (2020).
27. Ohi, M., Li, Y., Cheng, Y. & Walz, T. Negative staining and image classification — powerful tools in modern electron microscopy. *Biol. Proced. Online* **6**, 23–34 (2004).
28. Thomas, P. G. et al. Physiological numbers of CD4+ T cells generate weak recall responses following influenza virus challenge. *J. Immunol.* **184**, 1721–1727 (2010).
29. Chen, X. et al. The development and kinetics of functional antibody-dependent cell-mediated cytotoxicity (ADCC) to SARS-CoV-2 spike protein. *Virology* **559**, 1–9 (2021).
30. Tauzin, A. et al. A single dose of the SARS-CoV-2 vaccine BNT162b2 elicits Fc-mediated antibody effector functions and T cell responses. *Cell Host Microbe* **29**, 1137–1150 (2021).
31. Yu, Y. et al. Antibody-dependent cellular cytotoxicity response to SARS-CoV-2 in COVID-19 patients. *Signal Transduct. Target. Ther.* **6**, 346 (2021).
32. Guo, Y. et al. Elicitation of immunity in mice after immunization with the S2 subunit of the severe acute respiratory syndrome coronavirus. *DNA Cell Biol.* **24**, 510–515 (2005).
33. Zeng, F. et al. Quantitative comparison of the efficiency of antibodies against S1 and S2 subunit of SARS coronavirus spike protein in virus neutralization and blocking of receptor binding: Implications for the functional roles of S2 subunit. *FEBS Lett.* **580**, 5612–5620 (2006).
34. SARS-CoV Spike proteins expressed by the vaccinia virus tiantan strain: Secreted SQ protein induces robust neutralization antibody in mice. *Viral Immunol.* **22**, 57–66 (2009).
35. Tan, C. W. et al. Pan-sarbecovirus neutralizing antibodies in BNT162b2-immunized SARS-CoV-1 Survivors. *N. Engl. J. Med.* **385**, 1401–1406 (2021).
36. Zhang, Q. et al. A preliminary study in immune response of BALB/c and C57BL/6 mice with a locally allergic rhinitis model. *Am. J. Rhinol. Allergy* **37**, 410–418 (2023).
37. Zeng, M., Nourishirazi, E., Guinet, E. & Nouri-Shirazi, M. The genetic background influences the cellular and humoral immune responses to vaccines. *Clin. Exp. Immunol.* **186**, 190–204 (2016).
38. Adams, L. E. et al. Fc-mediated pan-sarbecovirus protection after alphavirus vector vaccination. *Cell Rep.* **42**, 112326 (2023).
39. Shiakolas, A. R. et al. Cross-reactive coronavirus antibodies with diverse epitope specificities and Fc effector functions. *Cell Rep. Med.* **2**, 100313 (2021).
40. Clark, J. et al. Protective effect and molecular mechanisms of human non-neutralizing cross-reactive spike antibodies elicited by SARS-CoV-2 mRNA vaccination. *Cell Reports* **43**, 114922 (2024).
41. Fairhead, M., Krndija, D., Lowe, E. D. & Howarth, M. Plug-and-play pairing via defined divalent streptavidins. *J. Mol. Biol.* **426**, 199–214 (2014).
42. Howarth, M. & Ting, A. Y. Imaging proteins in live mammalian cells with biotin ligase and monovalent streptavidin. *Nat. Protoc.* **3**, 534–545 (2008).
43. Pinto, D. et al. Broad betacoronavirus neutralization by a stem helix-specific human antibody. *Science* **373**, 1109–1116 (2021).
44. Mastronarde, D. N. Automated electron microscope tomography using robust prediction of specimen movements. *J. Struct. Biol.* **152**, 36–51 (2005).
45. Imai, M. et al. Characterization of a new SARS-CoV-2 variant that emerged in Brazil. *Proc. Natl. Acad Sci. USA* **118**, https://doi.org/10.1073/pnas.2106535118 (2021).
46. Changrob, S. et al. Cross-neutralization of emerging SARS-CoV-2 variants of concern by antibodies targeting distinct epitopes on spike. *mBio* **12**, e0297521 (2021).
47. Guthmiller, J. J., Dugan, H. L., Neu, K. E., Lan, L. Y. & Wilson, P. C. An efficient method to generate monoclonal antibodies from human B cells. *Methods Mol. Biol.* **1904**, 109–145 (2019).
48. Nie, J. et al. Quantification of SARS-CoV-2 neutralizing antibody by a pseudotyped virus-based assay. *Nat. Protoc.* **15**, 3699–3715 (2020).
49. Dugan, H. L. et al. Preexisting immunity shapes distinct antibody landscapes after influenza virus infection and vaccination in humans. *Sci. Transl. Med.* **12**, https://doi.org/10.1126/scitranslmed.abd3601 (2020).

Acknowledgements

Addgene plasmid #46367 (pET21-Streptavidin-Glutamate_Tag) was a gift from Mark Howarth. R.S.K. acknowledges support from the Garry Betty/V Foundation Chair Fund at the Georgia Institute of Technology. P.T., P.W., Y.K., and R.S.K. acknowledge support from the National Institute of Allergy and Infectious Diseases of the National Institutes of Health under Award Number P01AI165077. Y.K. also acknowledges support from the Japan Program for Infectious Diseases Research and Infrastructure (JP23wm0125002), and the University of Tokyo Pandemic Preparedness, Infection, and Advanced Research Center (UTOPIA) grant (JP233fa627001) from the Japan Agency for Medical Research and Development. We thank Thomas Miller for technical support with antigen-specific B cell sorting. The following reagent was obtained through BEI Resources, NIAID, NIH: Cercopithecus aethiops Kidney Epithelial Cells Expressing Transmembrane Protease, Serine 2 and Human Angiotensin-Converting Enzyme 2 (Vero E6-TMPRSS2-T2A-ACE2), NR-54970. This work was supported in part by the University of Wisconsin, Madison, the Department of Biochemistry at the University of Wisconsin, Madison, and public health service grant U24 GM139168 to E.R.W. from the NIH. We are grateful for the use of facilities and

instrumentation at the Cryo-EM Research Center in the Department of Biochemistry at the University of Wisconsin, Madison.

Author contributions

All authors P.J.H., R.S.P., K.L., A.Y., L.-A.V.d.V., J.E.Y., J.C., C.T., M.H., N.Z., E.R.W., P.T., P.C.W., Y.K., and R.S.K. were involved in the study design. P.J.H., R.S.P., K.L., A.Y., L.-A.V.d.V., J.E.Y., J.C., C.T., M.H., and N.Z. performed data collection and data analysis. P.J.H., R.S.P., A.Y., and R.S.K. wrote the manuscript. All authors read and approved the final manuscript.

Competing interests

The authors declare the following competing interests: Y.K. has received unrelated funding support from Daiichi Sankyo Pharmaceutical, Toyama Chemical, Tauns Laboratories, Inc., Shionogi & Co. LTD, Otsuka Pharmaceutical, KM Biologics, Kyoritsu Seiyaku, Shinya Corporation, and Fuji Rebio. The other authors declare no competing interests.

Additional information

Supplementary information The online version contains supplementary material available at https://doi.org/10.1038/s41467-025-55824-y.

Correspondence and requests for materials should be addressed to Yoshihiro Kawaoka or Ravi S. Kane.

Peer review information *Nature Communications* thanks Berend-Jan Bosch, and the other anonymous reviewer for their contribution to the peer review of this work. A peer review file is available.